

On the origin of almost-Gaussian scaling in asymptotically safe quantum gravity

Maximilian Becker,^{a,1} Alexander Kurov,^b and Frank Saueressig^a

^a*Institute for Mathematics, Astrophysics and Particle Physics (IMAPP), Radboud University, Heyendaalseweg 135, 6525 AJ Nijmegen, The Netherlands*

^b*Theory Department, Lebedev Physics Institute, Leninsky Prospect 53, Moscow 119991, Russia*

E-mail: M.Becker@hef.ru.nl, kurov@td.lpi.ru, F.Saueressig@hef.ru.nl

ABSTRACT: The gravitational asymptotic safety program envisions the high-energy completion of gravity through an interacting renormalization group fixed point, the Reuter fixed point. The predictive power of the construction is encoded in the spectrum of the stability matrix which is obtained from linearizing the renormalization group flow around this fixed point. A key result of the asymptotic safety program is that parts of this spectrum exhibits an almost-Gaussian scaling behavior, entailing that operators which are classically highly UV-irrelevant do not induce new free parameters. In this article, we track down the origin of this property by contrasting the structure of the stability matrix computed from the Wetterich equation and the Composite Operator equation within the realm of $f(R)$ -truncations. We show that the almost-Gaussian scaling is not linked to the classical part of the beta functions. It is a quantum-induced almost-Gaussian scaling originating from the quantum corrections in the flow equation. It relies on a subtle interplay among the analytic structure of the theory's two-point function and the way the Wetterich equation integrates out fluctuation modes. As a byproduct we determine the parts of the eigenmode spectrum which is robust with respect to changing the regularization procedure.

¹Corresponding author.

Contents

1	Introduction	1
2	Building the stability matrix at a RG fixed point	3
2.1	General structure of the beta functions	3
3	Almost-Gaussian scaling within $f(R)$-computations	8
3.1	Warm-up: the stability of Newton’s coupling	9
3.2	Polynomial $f(R)$ -truncations	11
4	Almost-Gaussian Scaling from the Quantum Corrections	17
5	Discussion and Conclusions	19
A	Calculation of γ_n^m for the operator family $\{\int d^d x \sqrt{g} R^n\}$	21
B	The flow equation for functional $f(R)$-truncations	24

1 Introduction

A key challenge in constructing a quantum field theory including gravitational interactions is the predictive power. This issue already appears in the perturbative quantization of the Einstein-Hilbert action where the negative mass dimension of Newton’s coupling leads to new divergences at each order in the loop expansion [1–4]. Removing these divergences requires the introduction of an infinite tower of counterterms. Following the observation that “any quantum field theory is renormalizable once all possible counterterms are taken into account”, this procedure may result in a perfectly viable quantum theory. Since each counterterm introduces a new free parameter, such a construction lacks predictive power though. This underlies the assessment that general relativity is an effective field theory [5] whose high-energy completion requires new physics.

The gravitational asymptotic safety program, recently reviewed in the book chapters [6–13] and text books [14, 15], offers an elegant way to equip this effective field theory with predictive power. The core of the program is an interacting fixed point of the theory’s Wilsonian renormalization group (RG) flow, the Reuter fixed point [16]. The asymptotic safety hypothesis then states that this fixed point controls the theory as the coarse-graining scale k is sent to infinity. The fact that this hypothesis supplies predictive power can then be seen as follows. By definition, the dependence of the dimensionless couplings $\{u^n\}$ on the coarse-graining scale is encoded in the beta functions

$$k\partial_k u^n(k) = \beta^n(u). \tag{1.1}$$

At a fixed point $\{u_*^n\}$ one has $\beta^n(u_*) = 0$, for all n . The RG flow in the vicinity of the fixed point can then be studied by linearizing the beta functions

$$k\partial_k u^n(k) = \sum_m (B_*)^n{}_m (u^m - u_*^m) + O((u^j - u_*^j)^2), \quad (B_*)^n{}_m = B^n{}_m(u_*) = \left. \frac{\partial \beta^n}{\partial u^m} \right|_{u=u_*}. \quad (1.2)$$

Here $B(u_*)$ is the stability matrix of the fixed point. The solutions of the linearized system are readily obtained in terms of the eigenvalues λ_I and corresponding (right) eigenvectors V_I of $B(u_*)$ and read

$$u^n(k) = u_*^n + \sum_J C_J V_J^n \left(\frac{k}{k_0} \right)^{\lambda_J}. \quad (1.3)$$

Here, the C_J are free coefficients specifying a solution and k_0 is an arbitrary reference scale. For eigendirections with $\text{Re}(\lambda_J) < 0$, the RG flow is dragged into the fixed point as $k \rightarrow \infty$. Conversely, eigendirections with $\text{Re}(\lambda_J) > 0$ repel the flow in this limit. In order to reach the fixed point, the integration constants along the UV-repulsive directions must be set to zero while the ones associated with the UV-attractive directions constitute free parameters. Hence the number of free parameters is determined by the spectrum of the stability matrix and equals the number of eigenvalues λ_I with negative real part. More precisely, the predictive power of asymptotic safety hinges on $\text{spec}(B_*)$, being bounded from below and containing a finite number of eigenvalues with $\text{Re} \lambda_I < 0$. Conventionally, $\text{spec}(B_*)$ is given in terms of the stability coefficients, also called the critical exponents, θ_I , defined as $\theta_I \equiv -\lambda_I$. Notably, $\text{spec}(B_*)$ is invariant under a redefinition of the couplings u^n [15]. For an asymptotically free theory, it agrees with (minus) the classical mass dimension of the operator. Since the bare action contains a finite number of relevant and marginal couplings only, predictive power is guaranteed. For the asymptotic safety construction, however, the presence of quantum fluctuations makes this feature highly non-trivial.

Determining the spectrum of B_* for the Reuter fixed point and its generalization to gravity-matter systems has been the subject of a vast body of research, see [17–28] for selected references. The primary approach builds on solving the Wetterich equation [16, 29–31], a formally exact functional renormalization group equation (FRGE) encoding the Wilsonian RG flow of the effective average action. The most comprehensive studies along these lines approximate Γ_k by a polynomial or a generic function in the Ricci scalar R and determine the beta functions (1.1) by projecting the RG flow onto a maximally symmetric spherical background [32–55]. Building on the functional $f(R)$ -truncations [33–37], Refs. [43, 56] considered polynomials up to order $N_{\text{prop}} = 70$ and observed that the eigenvalue spectrum of classically highly irrelevant operators essentially agrees with the classical scaling. This feature has been dubbed “almost-Gaussian scaling” and has been supported using various approximations of Γ_k also beyond the polynomial $f(R)$ -computations [22, 24, 25, 34, 57]. Taken together, these studies suggest that the number of free parameters associated with the Reuter fixed point could be as low as 3 or 4.

Complementary to solving the Wetterich equation, the stability matrix of a fixed point can also be approximated with a composite-operator equation (COE) [58–60]. This strategy has been applied to spacetime volumes and also to operators polynomial in the Ricci scalar

[61–63].¹ The $f(R)$ -type computations [61, 62] did not see any evidence for the almost Gaussian scaling behavior. In this case the addition of higher-order operators opened up new UV-relevant directions which is in variance with the results found by solving the Wetterich equation.

The goal of our work is to track down the origin of this mismatch. In this way, we are able to pinpoint the structural property of the Wetterich equation which underlies the almost Gaussian scaling of the operator spectrum at the Reuter fixed point. The direct comparison shows that this specific property is absent in the COE. This insight allows to tie the mismatch in the two approaches to the pole structure of the trace part of the graviton propagator on a constantly curved background. Moreover, it reveals that the “almost-Gaussian scaling” exhibited by the stability matrix is a genuine quantum phenomenon in the sense that it is not linked to the classical part of the beta functions. This analysis is an important step towards understanding one of the key properties of the gravitational asymptotic safety program, its predictive power. From a wider perspective, our results are also important when comparing the scaling dimensions computed from the composite operator equation to Monte Carlo simulations of the gravitational path integral within Euclidean Dynamical Triangulations (EDT) [67] and Causal Dynamical Triangulations (CDT) [68–70].

The remainder of this work is organized as follows. In Sec. 2, we derive a master equation giving the structure of the stability matrix at a generic fixed point. In Sec. 3, we compute the building blocks making up the master equation as they appear from solving the Wetterich equation and the composite operator equation for $f(R)$ -type operators on spherically symmetric backgrounds. In Sect. 4, we link these findings to the analytic structure of the two-point function and we end with a discussion and our conclusions in Sect. 5. In order to make our work self-contained some technical details on $f(R)$ -type truncations are given in Appendix A and B.

2 Building the stability matrix at a RG fixed point

2.1 General structure of the beta functions

The primary tool for investigating RG fixed points in quantum gravity is the effective average action Γ_k , a scale-dependent generalization of the ordinary effective action Γ . By construction, Γ_k provides a description of the effective dynamics which incorporates the effects of quantum fluctuations with momenta $p^2 \gtrsim k^2$ in its effective vertices. In the context of gravity, Γ_k depends on a background metric $\bar{g}_{\mu\nu}$ (which may be left unspecified), metric fluctuations $h_{\mu\nu}$ in this background, and ghost fields \bar{C}_μ, C^ν , arising from gauge-fixing the theory via the Faddeev-Popov construction. Hereby, the background metric $\bar{g}_{\mu\nu}$ and the fluctuations $h_{\mu\nu}$ combine to the full spacetime metric $g_{\mu\nu}$. The presence of a fixed, non-fluctuating background is essential to be able to define the coarse-graining scale k . The interaction monomials in Γ_k are taken to be invariant under (background) diffeomorphisms.

¹The initial idea of the COE is that it gives access to the anomalous scaling dimension of composite operators which do not naturally appear in the effective average action. This property has been exploited to study the anomalous scaling dimension of the geodesic distance [64–66].

Conceptually, the gravitational effective average action may be organized according to

$$\Gamma_k[h, \bar{C}, C; \bar{g}] = \bar{\Gamma}_k[g] + \hat{\Gamma}_k[h; \bar{g}] + \Gamma_k^{\text{ghost}}[h, \bar{C}, C; \bar{g}], \quad (2.1)$$

where $\bar{\Gamma}_k[g]$ is the “diagonal part” of Γ_k which depends on $\bar{g}_{\mu\nu}$ and $h_{\mu\nu}$ in the combination of $g_{\mu\nu}$ only, $\hat{\Gamma}_k[h; \bar{g}]$ is the off-diagonal part that also incorporates the gauge-fixing term, and $\Gamma_k^{\text{ghost}}[h, \bar{C}, C; \bar{g}]$ is the ghost-action. In addition, we may supplement the construction by (potentially non-local) “composite operators” $\{\tilde{\mathcal{O}}_n(k)\}$ coupled to their own sources ε_n ,

$$\Gamma_k[h, \bar{C}, C; \bar{g}; \varepsilon] = \Gamma_k[h, \bar{C}, C; \bar{g}] + \sum_n \varepsilon_n \tilde{\mathcal{O}}_n(k). \quad (2.2)$$

This extension coincides with the standard definition (2.1) for $\varepsilon_n = 0$.

The dependence of Γ_k on the coarse-graining scale k is governed by the Wetterich equation [16, 29–31],

$$\frac{d}{dt}\Gamma_k = \frac{1}{2}\text{STr} \left[\left(\Gamma_k^{(2)} + \mathcal{R}_k \right)^{-1} \frac{d}{dt}\mathcal{R}_k \right]. \quad (2.3)$$

Eq. (2.3) is a functional renormalization group equation (FRGE), in which STr denotes a sum over fluctuation modes (including a sum over all fields that Γ_k is a functional of) while $\Gamma_k^{(2)}$ denotes the second functional derivative of Γ_k with respect to these fluctuation fields. Moreover, \mathcal{R}_k is a regulator that equips fluctuations of low momenta with a k -dependent mass term, while it vanishes for fluctuations with $p^2 \gg k^2$. Further, we introduced the RG time $t \equiv \ln(k/k_0)$ for notational convenience.

Retaining the composite operators and expanding (2.3) to first order in ε_i gives the composite operator equation [59–62, 64–66],

$$\frac{d}{dt}\tilde{\mathcal{O}}_n(k) = -\frac{1}{2}\text{STr} \left[\left(\Gamma_k^{(2)} + \mathcal{R}_k \right)^{-1} \tilde{\mathcal{O}}_n^{(2)}(k) \left(\Gamma_k^{(2)} + \mathcal{R}_k \right)^{-1} \frac{d}{dt}\mathcal{R}_k \right]. \quad (2.4)$$

The main virtue of this equation is that it allows to study the scaling dimension of geometric quantities which typically do not appear in Γ_k . A prototypical example of the latter can be the geodesic distance between points studied in [64, 65]. The use of (2.4) requires information about the propagators $\left(\Gamma_k^{(2)} + \mathcal{R}_k \right)^{-1}$ though. This must be provided as an input, e.g., by solving the Wetterich equation appearing at zeroth order in ε_n . In the sequel, we will focus on composite operators which could also appear within $\Gamma_k[h, \bar{C}, C; \bar{g}]$.

The effective average action lives on the gravitational theory space \mathcal{T} . By definition, this linear space comprises all action functionals that can be constructed from the field content and are invariant under background diffeomorphism symmetry. Introducing a basis $\{\mathcal{O}_n\}$ on \mathcal{T} , we can expand,²

$$\Gamma_k[h; \bar{g}] = \sum_n \bar{u}^n(k) \mathcal{O}_n, \quad \tilde{\mathcal{O}}_m(k) = \sum_n \bar{Z}_m^n(k) \mathcal{O}_n. \quad (2.5)$$

²Two comments are in order. Firstly, one can obviously use different bases, say, $\{\mathcal{O}_n\}$ and $\{\mathcal{O}'_n\}$, to expand Γ_k and $\tilde{\mathcal{O}}_m$, respectively. In this work, however, we are only interested in the case $\mathcal{O}_n = \mathcal{O}'_n$. Secondly, the expansions (2.5) put a non-trivial constraint towards the basis $\{\mathcal{O}_n\}$, since our definition of Γ_k includes the gauge-fixing action which also depends on the theory’s couplings. While one might separate the gauge-fixing action from Γ_k in order to be able to choose the basis $\{\mathcal{O}_n\}$ more freely, here, we refrain from doing so for the sake of convenience. Moreover, in Sec. 3 below we will employ the physical gauge-fixing condition in which the gauge degrees of freedom do not source the anomalous scaling dimension of $\tilde{\mathcal{O}}_n$.

Here, $\bar{u}^n(k)$ and $\bar{Z}_m^n(k)$ are k -dependent, dimensionful couplings. Denoting the mass-dimension of the operators as $[\mathcal{O}_n] = -d_n$, it is convenient to introduce their dimensionless counterparts as

$$u^n(k) \equiv \bar{u}^n(k)k^{-d_n}, \quad \gamma_m^n(k) \equiv k^{d_m-d_n} [\bar{Z}^{-1} \partial_t \bar{Z}]_m^n. \quad (2.6)$$

The couplings u^n provide natural coordinates on the theory space, while $\gamma_m^n(k)$ encodes the anomalous scaling dimensions of the composite operators [60].

Plugging the expansion of Γ_k , Eq. (2.5), into the Wetterich equation (2.3), matching the coefficients of the basis elements \mathcal{O}_n , converting to dimensionless couplings (2.6), and solving the resulting system of equations for $\partial_t u^n(k)$, we arrive at the beta functions governing the dependence of the couplings $u^n(k)$ on the coarse graining scale,

$$\partial_t u^n(k) = \beta^n(u). \quad (2.7)$$

Analogously, the substitution of (2.5) into the COE (2.4) yields [59–62, 64–66],

$$\sum_m \gamma_n^m k^{d_m} \mathcal{O}_m = -\frac{1}{2} k^{d_n} \text{STr} \left[\left(\Gamma_k^{(2)} + \mathcal{R}_k \right)^{-1} \mathcal{O}_n^{(2)} \left(\Gamma_k^{(2)} + \mathcal{R}_k \right)^{-1} \frac{d}{dt} \mathcal{R}_k \right], \quad (2.8)$$

In this way, γ_n^m becomes a function of the couplings $u^n(k)$, i.e., $\gamma_n^m(k) \equiv \gamma_n^m(u(k))$. Note that γ_n^m also entails an dependence on the beta functions $\beta^n(u(k))$, due to the presence of $d\mathcal{R}_k/dt$ under the trace.

The goal of this work is to understand the predictive power of the Reuter fixed point based on abstract properties of two-point correlation functions. To do so, we compare the stability matrix B_* as in eq. (1.2) with scaling dimensions obtained from a composite-operator equation. Generally, one may interpret the eigenvalues of the matrix $-d_n \delta_n^m + \gamma_n^m$ as the full scaling dimensions of the operators $\{\mathcal{O}_n\}$. Thus, we have *two different methods at hand to evaluate critical exponents* – on the one hand, the (negative) eigenvalues of the stability matrix $(B_*^{\text{FRGE}})_n^m$ obtained from solving the Wetterich equation, and, on the other hand, the eigenvalues of $(B_*^{\text{COE}})_n^m = -d_n \delta_n^m + \gamma_n^m$ obtained from the composite operator equation.

Let us discuss the structure of the beta functions and the stability matrix in more detail. A critical element in their construction is the regulator \mathcal{R}_k which is conveniently written as³

$$\mathcal{R}_k(\bar{u}; z) = \mathcal{Z}(\bar{u}) R_k(z). \quad (2.9)$$

Here, $\mathcal{Z}(\bar{u})$ has a status of a wave function renormalization and carries a tensor structure with respect to internal field indices. It depends on t through the dimensionful couplings \bar{u} only. Furthermore, R_k is the scalar regulator. At the level of the Wetterich equation this \bar{u} -dependence is dictated by the choice of regularization procedure and is a generic feature [34]. At the level of the composite operator equation, there is more freedom since there is

³More precisely, in practice one will set $\mathcal{R}_k(u; z) = \sum_i \mathcal{Z}^{(i)}(\bar{u}) [P_k^i(z) - z^i]$, where $P_k(z) = z + R_k(z)$ and the index i runs from 1 to highest power of $\Delta = -\bar{D}^2$ appearing in $\Gamma_k^{(2)}$. For the sake of simplicity and without loss of generality, we will remain with the simplified form (2.9).

no direct relation between $\Gamma_k^{(2)}$ and \mathcal{O}_n which would fix such a dependence based on the composite operators under consideration. As a result of the decomposition (2.9), one has

$$\frac{d}{dt}\mathcal{R}_k(\bar{u}; z) = \left(\sum_n \frac{\partial \mathcal{Z}(\bar{u})}{\partial \bar{u}^n} \frac{\partial}{\partial t} \bar{u}^n \right) R_k(z) + \mathcal{Z}(\bar{u}) \left(\frac{\partial}{\partial t} R_k \right). \quad (2.10)$$

Substituting Eqs. (2.5) and (2.10) into the Wetterich equation, equating coefficients for the basis element \mathcal{O}_n , and retaining the LHS=RHS form yields

$$\partial_t u^n + d_n u^n = \omega^n(u) + \sum_m \tilde{\omega}^n{}_m(u) (\partial_t u^m + d_m u^m) \equiv \hat{\omega}^n(u; \partial_t u). \quad (2.11)$$

This structure disentangles the classical contributions (LHS) and the contributions of the quantum fluctuations (RHS) to the flow. We may think of the latter as a vector field $\hat{\omega}^n(u, \partial_t u)$ on the “theory’s configuration space”. The vector $\omega^n(u)$ and matrix $\tilde{\omega}^n{}_m(u)$ depend on the dimensionless couplings u^n , but not on their derivatives $\partial_t u^n$. We also observe that $\tilde{\omega}^n{}_m(u)$ may not depend on all couplings, but only those which appear in the regulator $\mathcal{R}_k(\bar{u})$. Explicit expressions for $\omega^n(u)$ and $\tilde{\omega}^n{}_m(u)$ can be given in terms of functional traces

$$\begin{aligned} \omega^n(u) &= \frac{1}{2} k^{-d_n} \text{STr} \left[\left(\Gamma_k^{(2)} + \mathcal{R}_k \right)^{-1} \mathcal{Z}(\bar{u}^i) \left(\frac{\partial}{\partial t} R_k \right) \right] \Big|_{\mathcal{O}_n}, \\ \tilde{\omega}^n{}_m(u) &= \frac{1}{2} k^{d_m - d_n} \text{STr} \left[\left(\Gamma_k^{(2)} + \mathcal{R}_k \right)^{-1} \frac{\partial \mathcal{Z}(\bar{u}^i)}{\partial \bar{u}^m} R_k \right] \Big|_{\mathcal{O}_n}. \end{aligned} \quad (2.12)$$

Here, we used the notation $|_{\mathcal{O}_n}$ to denote the projection of the trace onto the basis element \mathcal{O}_n and included factors of k in such a way that the LHS is given by dimensionless quantities. The beta functions (2.7) are then obtained by solving (2.11) for $\partial_t u^n$:

$$\beta^n(u) = -d_n u^n + \sum_m [(\mathbb{1} - \tilde{\omega}(u))^{-1}]^n{}_m \omega^m(u). \quad (2.13)$$

The beta functions (2.13) solve Eq. (2.11), i.e., they fulfill the identity

$$\beta^n(u) = -d_n u^n + \hat{\omega}^n(u, \beta(u)). \quad (2.14)$$

We can use this identity to organize the stability matrix obtained from Eq. (2.13). Thus, let us consider the (generalized) stability matrix

$$B^n{}_m(u) = \frac{\partial}{\partial u^m} \beta^n(u) \quad (2.15)$$

at a generic point along the RG trajectory,

$$\begin{aligned} B^n{}_m(u) &= -D^n{}_m + \frac{\partial}{\partial u^m} \hat{\omega}^n(u; \beta(u)) \\ &= -D^n{}_m + \frac{\partial}{\partial u^m} \hat{\omega}_0^n(u) + \sum_l \left[\left(\frac{\partial}{\partial u^m} \tilde{\omega}^n{}_l(u) \right) \beta^l(u) + \tilde{\omega}^n{}_l(u) B^l{}_m(u) \right]. \end{aligned} \quad (2.16)$$

Here, we have introduced the matrix of classical scaling dimensions, $D_m^n \equiv d_n \delta_m^n$, and the vector $\hat{\omega}_0^n(u) \equiv \hat{\omega}^n(u; 0)$. While it might be tempting to interpret the RHS of Eq. (2.16) as the classical scaling, in form of $-D_m^n$, and its appertaining quantum corrections, in form of $\partial_m \hat{\omega}^n$, one must take care with such interpretations at this stage, since $\partial_m \hat{\omega}^n$ depends on the classical scaling dimensions d_n and the stability matrix B itself. Solving Eq. (2.16) for B , one obviously has

$$B_m^n(u) = \sum_l [(\mathbb{1} - \tilde{\omega}(u))^{-1}]^n_l \left(-D_m^l + \frac{\partial \hat{\omega}_0^l(u)}{\partial u^m} + \sum_{l'} \frac{\partial \tilde{\omega}^{ll'}(u)}{\partial u^m} \beta^{l'}(u) \right). \quad (2.17)$$

In order to relate this expression for the stability matrix with the anomalous scaling dimensions obtained within the composite-operator formalism, let us re-arrange Eq. (2.16) one more time. Having in mind that $\hat{\omega}^n = k^{-d_n}(\text{RHS of Eq. (2.3)}|_{\mathcal{O}_n})$, it is a straightforward calculation to see that

$$\frac{\partial}{\partial u^m} \hat{\omega}^n(u; \beta(u)) = \gamma_m^n(u) + \tilde{\gamma}_m^n(u) + \sum_l \tilde{\omega}^{nl}(u) B_m^l(u), \quad (2.18)$$

where

$$\gamma_m^n(u) \equiv -\frac{1}{2} k^{d_m - d_n} \text{STr} \left[\left(\Gamma_k^{(2)} + \mathcal{R}_k \right)^{-1} \mathcal{O}_m^{(2)} \left(\Gamma_k^{(2)} + \mathcal{R}_k \right)^{-1} \frac{d}{dt} \mathcal{R}_k(\bar{u}(k)) \right] \Big|_{\mathcal{O}_n}, \quad (2.19)$$

is the anomalous-dimension matrix of Eq. (2.8) for the family of operators $\{\mathcal{O}_n\}$,⁴ and the matrix $\tilde{\gamma}_m^n(u)$ contains terms involving the \bar{u} -derivative of the regulator \mathcal{R}_k ,

$$\begin{aligned} \tilde{\gamma}_m^n(u) \equiv & -\frac{1}{2} k^{d_m - d_n} \text{STr} \left[\left(\Gamma_k^{(2)} + \mathcal{R}_k \right)^{-1} \left(\frac{\partial \mathcal{Z}(\bar{u})}{\partial \bar{u}^m} R_k \right) \left(\Gamma_k^{(2)} + \mathcal{R}_k \right)^{-1} \frac{d}{dt} \mathcal{R}_k(\bar{u}(k)) \right] \Big|_{\mathcal{O}_n} \\ & + \frac{1}{2} k^{d_m - d_n} \text{STr} \left[\left(\Gamma_k^{(2)} + \mathcal{R}_k \right)^{-1} \frac{\partial}{\partial \bar{u}^m} \left(\sum_l \frac{\partial \mathcal{Z}(\bar{u})}{\partial \bar{u}^l} d_l \bar{u}^l R_k + \mathcal{Z}(\bar{u}) \partial_t R_k \right) \right] \Big|_{\mathcal{O}_n}. \end{aligned} \quad (2.20)$$

In summary, for the stability matrix at the non-Gaussian fixed point (NGFP) we have established the formulae

$$\begin{aligned} (B_*)^n_m &= \sum_l [(\mathbb{1} - \tilde{\omega}(u_*))^{-1}]^n_l \left(-D_m^l + \frac{\partial \hat{\omega}_0^l(u)}{\partial u^m} \Big|_{u=u_*} \right) \\ &= \sum_l [(\mathbb{1} - \tilde{\omega}(u_*))^{-1}]^n_l \left(-D_m^l + \frac{\partial \omega^l(u)}{\partial u^m} + \frac{\partial}{\partial u^m} \left(\sum_{l'} \tilde{\omega}^{ll'} d_{l'} u^{l'} \right) \right) \Big|_{u=u_*} \\ &= \sum_l [(\mathbb{1} - \tilde{\omega}(u_*))^{-1}]^n_l \left(-D_m^l + \gamma_m^n(u_*) + \tilde{\gamma}_m^n(u_*) \right). \end{aligned} \quad (2.21)$$

⁴Note that Eq. (2.19) involves the relation $\mathcal{O}_m^{(2)} = \frac{\partial \Gamma_k^{(2)}}{\partial \bar{u}^m}$. As often the composite-operator equation (2.19) is evaluated for the case where $\{\mathcal{O}_n\}$ does not include gauge-fixing contributions, but where Γ_k does, we will denote γ as $\gamma^{\text{COE+GF}}$ and/or γ^{COE} to distinguish the results in which the gauge-fixing term is included into $\{\mathcal{O}_n\}$ or not.

Note that there is no simple identity expressing $\gamma_m^n, \tilde{\gamma}_m^n$ in terms of ω^n and $\tilde{\omega}_m^n$, individually. The second line of Eq. (2.21) should then be seen as a rearrangement of the first line, in terms of the piece given by γ_m^n , appearing in the COE, and contributions associated with the dependence of the regulator on the couplings \bar{u} , which have been collected in $\tilde{\gamma}_m^n$. Only their sum is related to $\hat{\omega}_0^n$, namely at the fixed point via $\partial\hat{\omega}_0^n/\partial u^m(u_*) = \gamma_m^n(u_*) + \tilde{\gamma}_m^n(u_*)$.

The formulae (2.21) are one of the main results of the present work. We stress that if the employed regulator \mathcal{R}_k in the Wetterich equation (2.3) was \bar{u} -independent (which in [10] is called a non-adaptive cutoff), one has $\tilde{\omega} = 0 = \tilde{\gamma}$ and the critical exponents of the theory would be given by $(B_*)^n_m = -D_m^n + \gamma_m^n(u_*)$. For this reasoning, one might naively expect this formula to give a generally “good” approximation of the stability matrix,

$$(B_*)^n_m \approx -D_m^n + \gamma_m^n(u_*), \quad (2.22)$$

even in the case in which the regulator is coupling-dependent. In particular, one would expect that “almost-Gaussian scaling” of the stability coefficients [24, 42, 43, 56] means that B_* is dominated by $-D_m^n$ with $\gamma_m^n(u_*)$ providing a small correction. With the examples below in Sec. 3, we will illustrate that this is not the case though. In other words, the matrices $\tilde{\gamma}_m^n(u_*)$ and especially $\tilde{\omega}_m^n(u_*)$ are crucial for determining the spectrum of the stability matrix B_* . This observation is important because in many systems, the critical exponents obtained from B_* constitute physical observables. (Whether this is actually the case for gravity is nevertheless up to debate, due to the complexity of constructing observables.) In non-gravitational settings, it is often customary to calculate the stability matrix for fixed values of the anomalous dimension, cf. [71], following Eq. (2.22). This raises the question about the physical relevance of the critical exponents obtained from $(B_*)^n_m$ versus those obtained from $-D_m^n + \gamma_m^n(u_*)$, in case there is no qualitative agreement among the two.

Lastly, we point out that for a fixed point corresponding to an asymptotically free theory, the quantum corrections to the stability matrix vanish ($\gamma = \tilde{\gamma} = \tilde{\omega} = 0$). In this case the stability coefficients agree with the mass dimensions of the couplings.

3 Almost-Gaussian scaling within $f(R)$ -computations

In this section, we will apply the general results obtained in Sec. 2 to the well-studied $f(R)$ -truncations [32–54]. Our analysis uses the standard computational framework employed in these works: all computations are carried out using the background of a maximally symmetric d -sphere S^d . Moreover, we employ the background approximation where the beta functions and anomalous dimensions are read off from the operators

$$\bar{\mathcal{O}}_n[\bar{g}] = \int d^d x \sqrt{\bar{g}} \bar{R}^n, \quad (3.1)$$

i.e., at zeroth order in the fluctuation fields. The scalar part of the regulator is chosen to be of Litim-type [72],

$$R_k(z) = (k^2 - z)\theta(k^2 - z), \quad (3.2)$$

where $\Theta(x)$ is the Heaviside step function. We first start with a one-dimensional projection in Sec. 3.1 before generalizing to the polynomial $f(R)$ -case in Sec. 3.2.

3.1 Warm-up: the stability of Newton's coupling

We start by illustrating the general structures derived in the previous section based on the background Einstein-Hilbert truncation [16, 73–76], adapting the derivation given in [15]. Thus, we solve the Wetterich equation (2.3) and the COE (2.8) based on the geometric operators

$$\begin{aligned}\mathcal{O}_1^{\text{COE}} &= \int d^d x \sqrt{\bar{g}} R, \\ \mathcal{O}_1^{\text{COE+GF}} &= \int d^d x \sqrt{\bar{g}} R + \frac{1}{2\alpha} \int d^d x \sqrt{\bar{g}} \bar{g}^{\mu\nu} F_\mu[h; \bar{g}] F_\nu[h; \bar{g}].\end{aligned}\tag{3.3}$$

These operators coincide with (3.1) once the fluctuation fields are set to zero. The gauge-condition is taken of the general form

$$F_\mu[h; \bar{g}] = \bar{D}^\nu h_{\mu\nu} - \frac{1+\beta}{d} \bar{D}_\mu h^\nu{}_\nu.\tag{3.4}$$

This subsection chooses harmonic gauge, $\alpha = 1, \beta = (d-2)/2$. The inclusion of the gauge-fixing term ensures that $\mathcal{O}_1^{(2)}$ depends on the background covariant derivative \bar{D}_μ in the form of the background Laplacian $\Delta = -\bar{g}^{\mu\nu} \bar{D}_\mu \bar{D}_\nu$ only.

In the first step, we project the Wetterich equation onto the subspace spanned by $\bar{\mathcal{O}}_1[\bar{g}]$. Thus, all vectors and matrices associated with this example are one-dimensional. Including the harmonic gauge-fixing condition, the corresponding ansatz for the effective average action reads

$$\bar{\Gamma}_k[g] + \hat{\Gamma}_k[h; \bar{g}] \simeq \bar{u}^1 \mathcal{O}_1^{\text{COE+GF}}, \quad \text{with} \quad u^1 \equiv k^{2-d} \bar{u}^1.\tag{3.5}$$

The coupling \bar{u}^1 is related to Newton's coupling G_k by $\bar{u}^1 = -\frac{1}{16\pi G_k}$ and we have $[\bar{u}^1] \equiv D_u = d-2 > 0$. Following the computation [15], the LHS=RHS form of the projected Wetterich equation, introduced in (2.11), is

$$\partial_t u^1 + D_u u^1 = \omega + \tilde{\omega}(u^1) (\partial_t u^1 + D_u u^1).\tag{3.6}$$

The vector $\omega(u)$ and matrix $\tilde{\omega}(u)$ given by $\omega = B_1$ and $\tilde{\omega}(u^1) = B_2/u^1$, with the constants

$$\begin{aligned}B_1 &= \frac{1}{(4\pi)^{d/2}} \frac{1}{12} \left(d(d-3) \Phi_{d/2-1}^1 - 6(d^2 - d + 4) \Phi_{d/2}^2 \right), \\ B_2 &= \frac{1}{(4\pi)^{d/2}} \frac{1}{24} \left(d(d+1) \tilde{\Phi}_{d/2-1}^1 - 6d(d-1) \tilde{\Phi}_{d/2}^2 \right).\end{aligned}\tag{3.7}$$

The dimensionless threshold functions $\Phi_n^p(w)$ and $\tilde{\Phi}_n^p(w)$ introduced in [16] are evaluated at vanishing argument and carry the dependence of the result on the choice of scalar regulator. For the Litim-type profile (3.2) they evaluate to

$$\Phi_n^p = \frac{1}{\Gamma(n+1)}, \quad \tilde{\Phi}_n^p = \frac{1}{\Gamma(n+2)}.\tag{3.8}$$

Notably, the present case is special in the sense that ω is independent of the coupling u^1 .

Solving (3.6) for $\partial_t u^1$ gives the beta function

$$\beta_u(u^1) = -D_u u^1 + \frac{\omega}{1 - \tilde{\omega}(u^1)}. \quad (3.9)$$

This beta function admits a single NGFP characterized by

$$u_*^1 = B_2 + \frac{B_1}{D_u}, \quad B_*^{\text{FRGE}} = -D_u + D_u^2 \frac{B_2}{B_1}. \quad (3.10)$$

Evaluating these expressions for $d = 4$ yields

$$u_*^1 \simeq -0.012, \quad B_*^{\text{FRGE}} = -2.09. \quad (3.11)$$

Thus, we encounter a NGFP situated at a positive Newton's coupling and a UV-attractive eigendirection.

In the next step, we compare this result to the one found in the composite operator approximation (2.22). Thus, we seek to find the anomalous scaling dimension of the operator $\bar{\mathcal{O}}_1[\bar{g}]$. Without the inclusion of the gauge-fixing term in (3.3), this computation has been carried out in [61], yielding

$$\begin{aligned} \gamma^{\text{COE}}(u_*^1) = & -\frac{1}{(4\pi)^{d/2}} \frac{1}{u_*^1} \left[\frac{1}{24} (d^3 + 9d^2 - 22d - 24) \left(\Phi_{d/2}^2 - \frac{1}{2}(2-d)\tilde{\Phi}_{d/2}^2 \right) \right. \\ & \left. - \frac{1}{2} (d^3 - 3d^2 + 4d - 8) \left(\Phi_{d/2+1}^3 - \frac{1}{2}(2-d)\tilde{\Phi}_{d/2+1}^3 \right) \right]. \end{aligned} \quad (3.12)$$

In comparison to the ‘‘exact definition’’ of γ , Eq. (2.19), this result neglects the contribution of the gauge-fixing terms in $\frac{\partial \Gamma_k^{(2)}}{\partial \bar{u}^m}$. Adding the gauge-fixing term (implementing harmonic gauge) changes this result to

$$\begin{aligned} \gamma^{\text{COE+GF}}(u_*^1) = & -\frac{1}{(4\pi)^{d/2}} \frac{1}{u_*^1} \left[\frac{1}{24} d(d^2 + 11d - 14) \left(\Phi_{d/2}^2 - \frac{1}{2}(2-d)\tilde{\Phi}_{d/2}^2 \right) \right. \\ & \left. - \frac{1}{2} d^2(d-1) \left(\Phi_{d/2+1}^3 - \frac{1}{2}(2-d)\tilde{\Phi}_{d/2+1}^3 \right) \right]. \end{aligned} \quad (3.13)$$

Using these results in (2.22) and specializing to $d = 4$ then yields

$$B_*^{\text{COE}} = -2 + \gamma^{\text{COE}}(u_*^1) = -1.91, \quad B_*^{\text{COE+GF}} = -2 + \gamma^{\text{COE+GF}}(u_*^1) = -1.94. \quad (3.14)$$

Hence, we again encounter a UV-attractive eigendirection. In both computations B_* is governed by the classical part $-D_u$ and receives a subleading correction from the quantum corrections. We also observe that there is a reasonable qualitative agreement between the exact projection and its approximation by the composite operator contribution. Subsequently, we will observe how this approximation becomes increasingly worse when going to increasing the order of the truncation.

3.2 Polynomial $f(R)$ -truncations

One of the most prominent results in the context of asymptotically safe quantum gravity is the “almost-Gaussian” scaling observed when considering polynomial $f(R)$ -truncations at sufficiently large order of the polynomials [42, 43]. This statement paraphrases that the spectrum of critical exponents $\{\theta_I^{\text{FRGE}} = -\lambda_I^{\text{FRGE}}\}$ of B_*^{FRGE} converges to the Gaussian scaling dimensions $\{d_I\}$. Hereby, the corrections to the first three classical scaling dimensions, $d_0 = 4$, $d_1 = 2$, and $d_2 = 0$ are such that the first two directions remain relevant, whereas the quantum corrections shift the third direction from a marginal to a relevant direction. All other directions remain irrelevant. For operators \mathcal{O}_n with sufficiently large value of n this is ensured by the aforementioned convergence pattern. Therewith, the polynomial $f(R)$ -truncation exhibits a three-dimensional UV-critical hypersurface.

In this section, we carry out a first reconnoitring study comparing the stability matrices at the fixed point obtained from the standard FRGE procedure for the $f(R)$ -truncation and the corresponding composite operator results. The FRGE computation is based on Eq. (2.21), i.e.,

$$\begin{aligned} (B_*^{\text{FRGE}})^n{}_m &= \sum_l [(\mathbb{1} - \tilde{\omega}(u_*))^{-1}]^n{}_l \left(-D_m^l + \frac{\partial \omega^l(u)}{\partial u^m} + \frac{\partial}{\partial u^m} \left(\sum_{l'} \tilde{\omega}^{l'} d_{l'} u^{l'} \right) \right) \Big|_{u=u_*} \\ &= \sum_l [(\mathbb{1} - \tilde{\omega}(u_*))^{-1}]^n{}_l \left(-D_m^l + \gamma_m{}^n(u_*) + \tilde{\gamma}_m{}^n(u_*) \right). \end{aligned} \quad (3.15)$$

The corresponding results for the scaling corrections emerging from the COE are obtained from Eq. (2.22), i.e.,

$$(B_*^{\text{COE}})^n{}_m = -D_m^n + \gamma_m{}^n(u_*). \quad (3.16)$$

This comparison thus boils down to the question whether we may neglect the contributions of the matrices $\tilde{\omega}_m{}^n(u_*)$ and $\tilde{\gamma}_m{}^n(u_*)$. If we do so for the contribution of $\tilde{\gamma}_m{}^n(u_*)$, we may think of the matrix $\tilde{\omega}_m{}^n(u_*)$ as translating between the two approximations.

We start by analyzing Eq. (3.15). For functional $f(R)$ -truncations the ingredients in Eq. (2.1) take the form

$$\begin{aligned} \bar{\Gamma}_k[g] &= \int d^d x \sqrt{\bar{g}} f_k(R) = \int d^d x \sqrt{\bar{g}} k^d \mathcal{F}_k(\rho), \\ \hat{\Gamma}[h; \bar{g}] &= \frac{1}{2\alpha} \int d^d x \sqrt{\bar{g}} \bar{g}^{\mu\nu} F_\mu[h; \bar{g}] F_\nu[h; \bar{g}]. \end{aligned} \quad (3.17)$$

Here $f_k(R)$ is a generic, k -dependent function of the scalar curvature R with dimensionless counterparts, $\mathcal{F}_k(\rho) = k^{-d} f_k(R)$ and $\rho = k^{-2} R$. Supplementing (3.17) by the corresponding ghost action and substituting the result into the Wetterich equation results in a partial differential equation governing the functional form of $\mathcal{F}_k(\rho)$. There are several incarnations of this equation which differ by the treatment of the discrete modes appearing on spherical backgrounds [10].

The technical construction of the flow equation for $f(R)$ -truncations implements the York decomposition [77, 78] of the fluctuation fields

$$h_{\mu\nu} = h_{\mu\nu}^{\text{TT}} + \bar{D}_\mu \xi_\nu + \bar{D}_\nu \xi_\mu + \bar{D}_\mu \bar{D}_\nu \sigma - \frac{1}{d} \bar{g}_{\mu\nu} \bar{D}^2 \sigma + \frac{1}{d} \bar{g}_{\mu\nu} h. \quad (3.18)$$

Here $h_{\mu\nu}^{\text{TT}}$ is the transverse-traceless (TT) part, $\hat{\xi}_\mu$ is the transverse vector field of the longitudinal part of $h_{\mu\nu}$, σ is the corresponding longitudinal scalar, and h is the trace part. The component fields are subject to the constraints

$$\bar{D}^\mu h_{\mu\nu}^{\text{TT}} = 0, \quad \bar{g}^{\mu\nu} h_{\mu\nu}^{\text{TT}} = 0, \quad \bar{D}_\mu \xi^\mu = 0, \quad \bar{g}^{\mu\nu} h_{\mu\nu}^{\text{TT}} = h. \quad (3.19)$$

The fields are re-scaled to be orthonormal on Einstein spaces,

$$\hat{\xi}_\mu = (2(\Delta - \bar{R}/d))^{1/2} \xi_\mu, \quad \hat{\sigma} = \left(\frac{d-1}{d} \Delta (\Delta - \bar{R}/(d-1)) \right)^{1/2} \sigma, \quad \hat{h} = \frac{1}{\sqrt{d}} h, \quad (3.20)$$

which also accounts for the Jacobians arising from the decomposition (3.18).

Owed to the higher-derivative terms generated by $\bar{\Gamma}_k$ it turns out to be convenient to restrict (3.17) to Landau-type gauges, which fix $\beta = 0$ and take the limit $\alpha \rightarrow 0$ once all ingredients in the traces are computed. The ghost-sector arising from this ‘‘physical gauge’’ follows [33]. This choice leads to a number of simplifications. Firstly, the matrix $(\Gamma_k^{(2)} + \mathcal{R}_k)$ becomes diagonal in field space. Secondly, the contributions of the unphysical transverse vector field ξ_μ and the unphysical scalar field σ become independent of the function $f_k(R)$. This is readily deduced by analyzing the α -dependence of the decomposed propagator (see Table 1 in [33] and Eqs. (97)-(99) of [34]). Conversely, the matrix elements for the transverse traceless and \hat{h} -fluctuations appearing in $(\Gamma_k^{(2)} + \mathcal{R}_k)$ are solely governed by $\bar{\Gamma}_k[g]$. Specifying to the Litim-type regulator, they read [34]

$$\begin{aligned} (\Gamma_{k,\text{TT}}^{(2)} + \mathcal{R}_{k,\text{TT}}) &= -\frac{1}{2} \left[\left(k^2 - \frac{2(d-2)}{d(d-1)} \bar{R} \right) f'_k + f_k \right] \mathbb{1}_{\text{TT}}, \\ (\Gamma_{k,\hat{h}\hat{h}}^{(2)} + \mathcal{R}_{k,\hat{h}\hat{h}}) &= \frac{d-2}{4} \left[\frac{4(d-1)^2}{d(d-2)} f''_k \left(k^2 - \frac{\bar{R}}{d-1} \right)^2 \right. \\ &\quad \left. + \frac{2(d-1)}{d} f'_k \left(k^2 - \frac{\bar{R}}{d-1} \right) - \frac{2\bar{R}}{d} f'_k + f_k \right]. \end{aligned} \quad (3.21)$$

Here, $\mathbb{1}_{\text{TT}}$ is the identity on the space of transverse-traceless fields, $f'_k(R) = \partial_R f_k(R)$, and we adopt an identical notation for the dimensionless functions $\mathcal{F}'_k(\rho) = \partial_\rho \mathcal{F}_k(\rho)$. The explicit form of corresponding matrix element of the regulator \mathcal{R}_k arising from implementing the adaptive cutoff $\Delta \mapsto \Delta + R_k$ is

$$\begin{aligned} \mathcal{R}_{k,\text{TT}} &= -\frac{1}{2} f'_k R_k \mathbb{1}_{\text{TT}}, \\ \mathcal{R}_{k,\hat{h}\hat{h}} &= \frac{d-1}{2d} \left[(d-2) f'_k + 2(d-1) f''_k (2\Delta + R_k) - 4 f''_k \bar{R} \right] R_k. \end{aligned} \quad (3.22)$$

The Wetterich equation takes the schematic form

$$\begin{aligned} \frac{d}{dt} \bar{\Gamma}_k &= \frac{1}{2} \text{Tr}_{\text{TT}} \left[\left(\bar{\Gamma}_{k,\text{TT}}^{(2)} + \mathcal{R}_{k,\text{TT}} \right)^{-1} \frac{d}{dt} \mathcal{R}_{k,\text{TT}} \right] + \frac{1}{2} \text{Tr}_S \left[\left(\bar{\Gamma}_{k,\hat{h}\hat{h}}^{(2)} + \mathcal{R}_{k,\hat{h}\hat{h}} \right)^{-1} \frac{d}{dt} \mathcal{R}_{k,\hat{h}\hat{h}} \right] \\ &+ \bar{\Gamma}_k\text{-independent terms}, \end{aligned} \quad (3.23)$$

where the $\bar{\Gamma}_k$ -independent terms are due to the Fadeev-Popov ghosts and the contributions of the ξ_μ and σ modes. Owing to the presence of the higher-derivative terms, the regulator does not obey the simple factorization (2.9). Nevertheless, one is able to separate the trace contributions into parts associated with the regulator and the couplings appearing within (3.22). The result of this computation is rather lengthy and given as Eq. (B.1) of Appendix B.

We then project Eq. (3.23) onto the basis (3.1). Introducing the dimensionless volume $\tilde{V} = k^d \int d^d x \sqrt{g} \propto \rho^{-d/2}$, the LHS of Eq. (3.23) is

$$\frac{d}{dt} \bar{\Gamma}_k = \tilde{V} \{ (\partial_t \mathcal{F}_k)(\rho) + d \mathcal{F}_k(\rho) - 2\rho \mathcal{F}'_k(\rho) \}. \quad (3.24)$$

Since in general the regulator is of the form $\mathcal{R}_k = \mathcal{R}_k[f'_k, f''_k]$, the RHS can be written as

$$\text{RHS} = \tilde{V} \left\{ I_0[\mathcal{F}_k](\rho) + \left(k^{-d+2} \frac{d}{dt} f'_k \right) (\rho) I_1[\mathcal{F}_k](\rho) + \left(k^{-d+4} \frac{d}{dt} f''_k \right) (\rho) I_2[\mathcal{F}_k](\rho) \right\}. \quad (3.25)$$

Each function I_0 , I_1 , and I_2 contains contribution from the TT- and trace-sector as well as from the $f_k(R)$ -independent terms. For details, we refer the reader to [43].

The transition from the functional to the polynomial form of Eqs. (3.24) and (3.25) uses the expansion

$$f_k(R) = \sum_{n=0}^{N_{\text{prop}}} \bar{u}^n(k) R^n, \quad \mathcal{F}_k(\rho) = \sum_{n=0}^{N_{\text{prop}}} u^n(k) \rho^n, \quad (3.26)$$

where the polynomials are truncated at N_{prop} . The LHS given in Eq. (3.24) then becomes

$$\frac{d}{dt} \bar{\Gamma}_k = \tilde{V} \sum_{n=0}^{N_{\text{prop}}} \{ \partial_t u^n + d_n u^n \} \rho^n, \quad (3.27)$$

with $d_n = d - 2n$ the canonical mass dimension of the dimensionful couplings \bar{u}^n . Projecting the RHS, Eq. (3.25), onto the operators (3.1) is akin to Taylor-expanding this RHS around $\rho = 0$,

$$I_0[\mathcal{F}_k](\rho) = \sum_n \omega^n(u) \rho^n, \quad (3.28)$$

and

$$\left(k^{-d+2} \frac{d}{dt} f'_k \right) (\rho) I_1[\mathcal{F}_k](\rho) + \left(k^{-d+4} \frac{d}{dt} f''_k \right) (\rho) I_2[\mathcal{F}_k](\rho) = \sum_{n,m} \tilde{\omega}^n_m(u) [\partial_t u^m + d_m u^m] \rho^n. \quad (3.29)$$

Since the LHS of Eq. (3.29) is independent of \bar{u}^0 , we have $\tilde{\omega}^n_0 \equiv 0$. The structure highlighted on its RHS then arises from the expansions

$$\begin{aligned} \left(k^{-d+2} \frac{d}{dt} f'_k \right) (\rho) &= \sum_{n=0} n [\partial_t u^n + d_n u^n] \rho^{n-1}, \\ \left(k^{-d+4} \frac{d}{dt} f''_k \right) (\rho) &= \sum_{n=0} n(n-1) [\partial_t u^n + d_n u^n] \rho^{n-2}. \end{aligned} \quad (3.30)$$

In this way, the definitions of the vector $\omega^n(u)$ and the matrix $\tilde{\omega}^n_m(u)$ agree precisely with the definitions given in Eq. (2.12). The explicit form for $\omega^n(u)$ and $\tilde{\omega}^n_m(u)$ are readily obtained using Computer-Algebra-Systems.

Combining these results with Eqs. (2.13) and (2.21), it is straightforward to obtain fixed points $\{u_*^n\}$ as well as the stability matrix B_*^{FRGE} . In the present work, for the case $d = 4$, we will employ the particular fixed point values $\{u_*^n\}$ obtained in [34]. For $N_{\text{prop}} = 8$ these are given by (see [34, Table III]):

$$(u_*^0, u_*^1, \dots, u_*^8) = 10^{-3} (5.066, -20.748, 0.088, -8.581, -8.926, -6.808, 1.165, 6.196, 4.695). \quad (3.31)$$

When using fixed point values for propagators with $N_{\text{prop}} < 8$, we will simply cut off the list (3.31) at the corresponding value instead of using the fixed point values obtained from the $N_{\text{prop}} < 8$ -truncation. We do so because the list (3.31) represents a more accurate approximation of the fixed point position $\{u_*\}$ also at lower orders of the truncation.

In order to compare these results with the scaling corrections obtained from γ_m^n for the family of composite operators $\{\mathcal{O}_n = \int d^d x \sqrt{g} R^n \mid n = 0, 1, \dots, N_{\text{scal}}\}$, we must evaluate Eq. (2.8). In this case only the TT- and trace-modes contribute,

$$\sum_m \gamma_n^m(u) \rho^m =: I_1 + I_2, \quad (3.32)$$

where

$$\begin{aligned} I_1 &:= -\frac{k^{d_n}}{2\tilde{V}} \text{Tr}_{\text{TT}} \left[\left(\frac{d}{dt} \mathcal{R}_{k,\text{TT}} \right) \left(\bar{\Gamma}_{k,\text{TT}}^{(2)} + \mathcal{R}_{k,\text{TT}} \right)^{-1} \mathcal{O}_n^{(2)}{}_{\text{TT}} \left(\bar{\Gamma}_{k,\text{TT}}^{(2)} + \mathcal{R}_{k,\text{TT}} \right)^{-1} \right], \\ I_2 &:= -\frac{k^{d_n}}{2\tilde{V}} \text{Tr}_{\text{S}} \left[\left(\frac{d}{dt} \mathcal{R}_{k,\hat{h}\hat{h}} \right) \left(\bar{\Gamma}_{k,\hat{h}\hat{h}}^{(2)} + \mathcal{R}_{k,\hat{h}\hat{h}} \right)^{-1} \mathcal{O}_n^{(2)}{}_{\hat{h}\hat{h}} \left(\bar{\Gamma}_{k,\hat{h}\hat{h}}^{(2)} + \mathcal{R}_{k,\hat{h}\hat{h}} \right)^{-1} \right]. \end{aligned} \quad (3.33)$$

In order to read off the anomalous-dimension matrix γ_n^m , we have to calculate the two traces I_1 and I_2 that built the RHS of Eq. (3.32), and Taylor-expand them in powers of ρ . For the propagators arising from the Einstein-Hilbert truncation, this computation has been carried out in [61, 62]. In order to be able to compare to the polynomial $f(R)$ -truncations of the Wetterich equation, we extend this study to the propagators (3.21) retaining terms in the expansion (3.26) up to N_{prop} . Since this particular calculation has not been performed in the literature before, we have collected the details in Appendix A. Note that the composite operator equation (3.32) allows us to truncate the operator bases $\{\mathcal{O}_n = \int d^d x \sqrt{g} R^n, n = 0, \dots, N_{\text{scal}}\}$ and the propagator at different values. These are then denoted by N_{scal} and N_{prop} , respectively. The FRGE formalism above obviously only

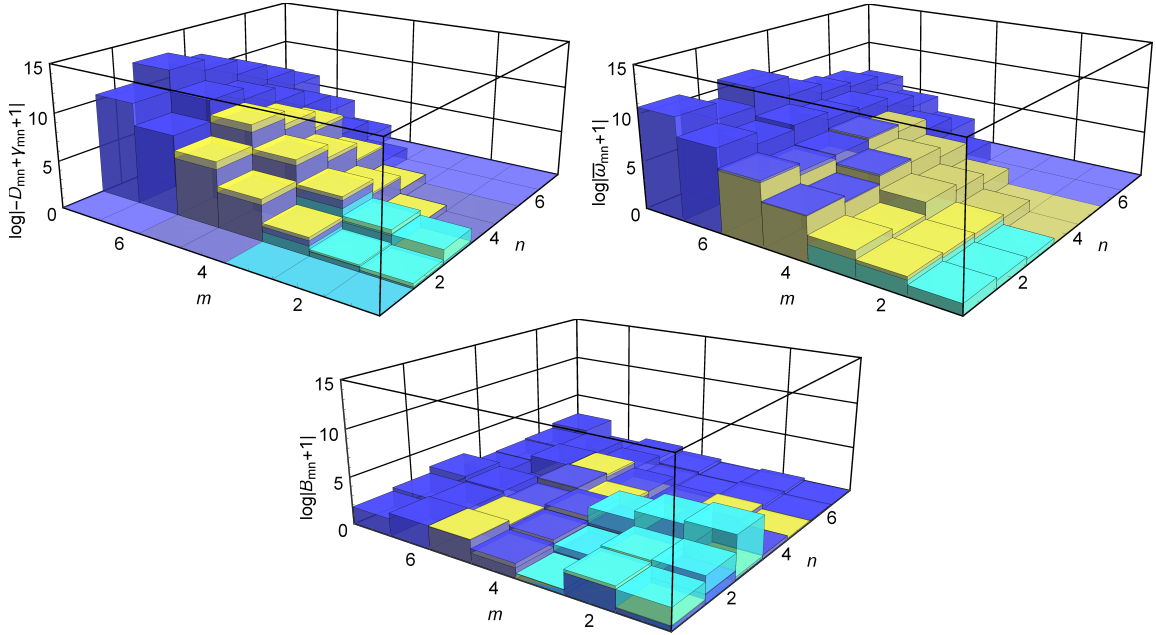


Figure 1. Illustration of the size of the matrix entries appearing in $-D + \gamma^T(u_*)$ (upper left), $\tilde{\omega}(u_*)$ (upper right) and the stability matrix B_* (lower row) entering the master equation (2.21) on a logarithmic scale. The colors refer to the systems with $N_{\text{scal}} = N_{\text{prop}} = 3$ (cyan), $N_{\text{scal}} = N_{\text{prop}} = 5$ (yellow), and $N_{\text{scal}} = N_{\text{prop}} = 7$ (blue). The top lines illustrate that the size of the entries grow with the matrix indices m, n . At the level of the stability matrix, it is the interplay between the two contributions in the top row, which significantly reduces the size of the coefficients appearing in Eq. (3.15).

admits the case $N_{\text{scal}} = N_{\text{prop}}$. As for the case of the stability matrix B_*^{FRGE} , results for γ_n^m are readily obtained using Computer-Algebra-Software.

At this point, we are ready to compare the stability matrices (3.15) and (3.16). For concreteness, we limit the discussion to $d = 4$. Inspecting Eq. (3.16), one might naively infer from here that the spectrum of B_*^{COE} is quite similar to that of B_*^{FRGE} , with the anomalous scaling dimensions $\gamma_m^n(u_*)$ providing corrections to $-D_m^n$ that become smaller and smaller as $N_{\text{prop}} = N_{\text{scal}} \rightarrow \infty$. In Fig. 1, we illustrate the entries of their building blocks $-D + \gamma^T$ (top left diagram), $\tilde{\omega}$ (top right diagram) and B_* (bottom) for various values of N_{scal} and N_{prop} on a logarithmic scale. This decomposition actually establishes that the opposite is true: The entries of $\gamma_m^n(u_*)$ grow exponentially as $N_{\text{prop}} = N_{\text{scal}} \rightarrow \infty$. In addition, Fig. 1 also depicts that the proliferation of matrix entries is not limited to $\gamma_m^n(u_*)$, but also happens in an almost identical fashion for $\tilde{\omega}_m^n(u_*)$. It is striking to observe how in Eq. (2.21) these two rampant, and seemingly unphysical, matrices combine to B_*^{FRGE} whose entries' magnitudes are in perfect unison with $-D_m^n$.

As a consequence of the exponential growths in the quantum parts, the spectra of B_*^{COE} and B_*^{FRGE} disagree even at a qualitative level, cf. Table 1. Qualitative agreement – in terms of an agreement on the sign of the critical exponents – is only assured for small-size truncations up to $N_{\text{prop}} = N_{\text{scal}} = 2$. For larger-size truncations, the entries of $\gamma_m^n(u_*)$

N_{scal}	N_{prop}		λ_0	λ_1	λ_2	λ_3	λ_4	λ_5	λ_6
		$-D$	-4	-2	0	2	4	6	8
0	≥ 3	B_*^{COE}	-2.04						
1	1	B_*^{FRGE}		-2.09					
		B_*^{COE}		-1.91					
		$B_*^{\text{COE+GF}}$		-1.94					
2	2	B_*^{FRGE}	-27.02	$-1.26 \pm 2.45i$					
		B_*^{COE}		$-4.06 \pm 1.38i$	-0.89				
4	4	B_*^{FRGE}	$-2.84 \pm 2.42i$		-1.54	4.27	5.09		
		B_*^{COE}	$-3.07 \pm 2.79i$		3.83	49.1	290.7		
6	6	B_*^{FRGE}	$-2.39 \pm 2.38i$		-1.51	4.16	$4.68 \pm 6.09i$		8.68
		B_*^{COE}	$-21.30 \pm 22.10i$		-4.53	$0.66 \pm 2.35i$	329.0		954.9
		B_*^{loc}	$-(26 + 4.4d_1)10^{10}$		-6	-4	-2	0	
6	2	B_*^{FRGE}		-	-	-	-	-	-
		B_*^{COE}		$-11.74 \pm 19.49i$	-9.80	$-2.41 \pm 1.88i$	-0.15		3.64

Table 1. Illustration of the spectral properties of the matrices B_*^{FRGE} and B_*^{COE} for several values of N_{scal} and N_{prop} . The first line (classical scaling) gives the entries of $-D$. Complex eigenvalues are presented pairwise in a double-column entry. The case $N_{\text{scal}} = N_{\text{prop}} = 1$ summarizes the results of Sect. 3.1 while the lower entries compare the spectra of the stability matrix obtained from solving the FRGE and COE for polynomial $f(R)$ -truncations. Note that the definition of B_*^{FRGE} entails that $N_{\text{scal}} = N_{\text{prop}}$. The results from the “localization approximation” (loc) are referenced from Eq. (4.7).

reach a size that distorts the spectrum of B_*^{COE} altogether, with the quantum corrections exceeding the classical (Gaussian) scaling dimensions by orders of magnitude. In Table 1 this becomes evidently clear for $N_{\text{prop}} = N_{\text{scal}} = 6$. These corrections surely seem intuitively anomalous and far from a physically reliable estimate. This is a paradoxical situation since, as we had mentioned earlier on, there exist plenty of physical systems, e.g. in the realm of condensed matter physics, for which the critical exponents emanating from B_*^{COE} constitute actual physical observables.

As regards to observables, we would like to point out another striking results that Table 1 exhibits. For geometrical operators depending on some characteristic scale, the (negative) eigenvalues of $-D + \gamma$ can also be interpreted as the geometric scaling dimensions of these operators. In case of a single-operator approximation given by the spacetime volume \mathcal{O}_0 (i.e., $N_{\text{scal}} = 0$), we find dimensional reduction of its scaling dimension from classically 4 down to 2.04. Albeit a gauge-dependent result, this strikingly confirms the dimensional reduction of spacetime in the UV from 4 to 2 dimensions that has already been observed in a variety of settings [79], including Asymptotic Safety [80] and CDT [69].

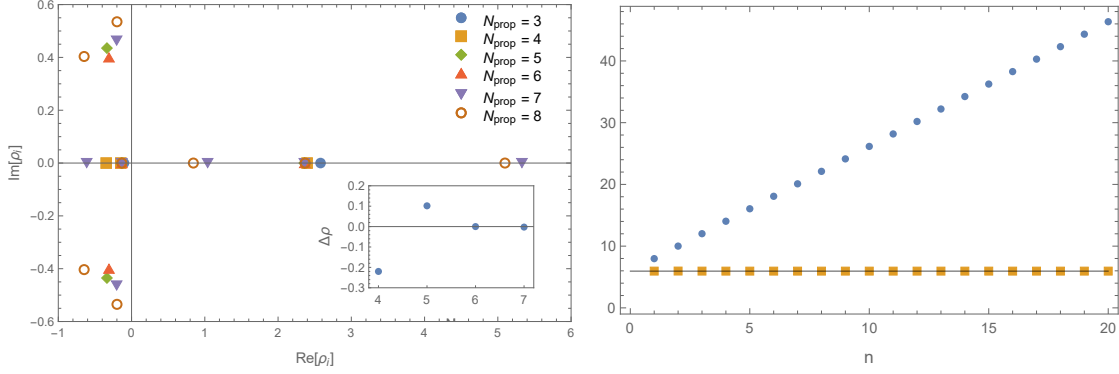


Figure 2. Illustration of the analytic structure of $(\Gamma_{k, \hat{h}\hat{h}}^{(2)} + \mathcal{R}_{k, \hat{h}\hat{h}})$ (left) and the coefficients appearing in the series expansion eq. (4.3) (right).

4 Almost-Gaussian Scaling from the Quantum Corrections

The take-away message from Fig. 1 is that the spectrum of the stability matrix is essentially determined by the interplay between the quantum contributions to Eq. (3.15). At this point, it is highly interesting to understand the mechanism that actually underlies our findings in Table 1. The key ingredient is the (regularized) two-point correlation function $(\Gamma_k^{(2)} + \mathcal{R}_k)$. In general, this operator is matrix-valued in field space. A detailed inspection of this matrix shows, that it is only one specific matrix element which drives the mechanism, the one associated with the trace part \hat{h} appearing in the decomposition (3.18).

The first step is to understand the root structure of (3.21). For this purpose, we restrict to $d = 4$, substitute the expansions of $f(\bar{R})$ up to $N_{\text{prop}} = \{3, 4, 5, 6, 7, 8\}$, and convert to dimensionless variables. Substituting the fixed point position (3.31), this leads to a polynomial of order N_{prop} in the dimensionless curvature ρ . For $N_{\text{prop}} = 8$, the resulting expression is given by

$$(\Gamma_{k, \hat{h}\hat{h}}^{(2)} + \mathcal{R}_{k, \hat{h}\hat{h}})(u_*) = \frac{k^4}{4} (0.197\rho^8 - 1.279\rho^7 + 0.958\rho^6 + 2.072\rho^5 + 0.976\rho^4 - 0.707\rho^3 - 0.732\rho^2 - 0.464\rho - 0.051). \quad (4.1)$$

The roots of these polynomials are easily found numerically and depicted in the left panel of Fig. 2. Increasing N_{prop} adds a new root in each step. The most important one is the one which is closest to the expansion point $\rho = 0$. This root appears at $N_{\text{prop}} = 3$ and remains stable when N_{prop} is increased. For $N_{\text{prop}} = 8$, its position is given by

$$\rho_0^{N_{\text{prop}}=8} = -0.133. \quad (4.2)$$

The relative distance between the root found at lower orders, $\Delta\rho \equiv \frac{\rho_0^{N_{\text{prop}}=n} - \rho_0^{N_{\text{prop}}=8}}{\rho_0^{N_{\text{prop}}=8}}$, is displayed in the inset, demonstrating the stability of the root with respect to increase of N_{prop} . The corresponding analysis in the transverse-traceless sector shows that in this case the root closest to the origin is at $|\rho_{\hat{h}\hat{h}}^{N_{\text{prop}}=8}| \approx 0.66$.

It turns out that it is the root (4.2) that dominates the expansion of the flow equations in the dimensionless Ricci scalar ρ . This is seen as follows. The Wetterich and composite

operator equations contain the inverse of the two-point function. For the specific gauge choice the matrix $(\Gamma_k^{(2)} + \mathcal{R}_k)$ diagonalizes, so the inverse contains the inverse of $(\Gamma_{k,\hat{h}\hat{h}}^{(2)} + \mathcal{R}_{k,\hat{h}\hat{h}})$ which is expanded at $\rho = 0$. Evaluating this expansion at the fixed point u_* yields

$$(\Gamma_{k,\hat{h}\hat{h}}^{(2)} + \mathcal{R}_{k,\hat{h}\hat{h}})^{-1}(u_*) = \sum_n \tau^n(u_*) \rho^n. \quad (4.3)$$

The expansion coefficients $\tau^n(u_*)$ are illustrated in the right panel of Fig. 2. Here the blue dots correspond to $\log |\tau^n(u_*)|$ while the orange plots display $\log |\tau^n(u_*) (\rho_0^{N_{\text{prop}}=8})^n|$. Owing to the pole in the complex unit circle, the coefficients grow exponentially. This is illustrated by the blue dots. The orange points show that the growth is controlled by $\rho_0^{N_{\text{prop}}=8}$ already for low values of n . Thus, we recover the familiar result that the growth of the expansion coefficients is controlled by the root closest to the expansion point⁵

$$\lim_{n \rightarrow \infty} \left| \frac{\tau^{n+1}(u_*)}{\tau^n(u_*)} \right| = \frac{1}{\rho_0^{N_{\text{prop}}=8}}. \quad (4.4)$$

As shown in the right diagram of Fig. 2, this relation is already fulfilled to very good accuracy at low values $n \simeq 10$. It is straightforward to repeat this analysis for the other matrix elements appearing in $(\Gamma_k^{(2)} + \mathcal{R}_k)$. Since the root in the scalar sector is the one closest to the expansion point, the expansion coefficients in this sector exhibit the fastest growth and therefore determine the structure of the flow equation at large N_{prop} . This feature propagates into the entries of $\omega^n(u_*)$ and $\tilde{\omega}_m^n(u_*)$ and also to $\gamma_m^n(u_*)$ and $\tilde{\gamma}_m^n(u_*)$.

The exponential growth of the expansion coefficients (4.3) entails that it is the *scalar trace which dominates* the beta functions for couplings \bar{u}^n with n sufficiently large. In particular, the classical contributions originating from the LHS of the flow equation (encoded in D) are negligible. This suggests that for sufficiently large values of n , a good approximation of the flow is given by

$$\frac{1}{2} \text{Tr}_S \left[\left(\Gamma_{k,\hat{h}\hat{h}}^{(2)} + \mathcal{R}_{k,\hat{h}\hat{h}} \right)^{-1} \left(\frac{d}{dt} \mathcal{R}_{k,\hat{h}\hat{h}} \right) \right] \approx 0. \quad (4.5)$$

We will call this the “localization” (loc) approximation, since the analytic structure of the propagator essentially localizes the contributions of the RG flow in one single sector.

Since (4.5) is a pure quantum expression, this immediately raises the puzzle about how the localization approximation may recover any knowledge about the classical scaling dimensions d_{u^n} . In order to answer this question, let us evaluate the RG-time derivative of (3.22),

$$\begin{aligned} \frac{d}{dt} \mathcal{R}_{k,\hat{h}\hat{h}} = \frac{3}{4} \left\{ [f'_k + 6f''_k(\Delta + R_k) - 2f''_k \bar{R}] \partial_t R_k \right. \\ \left. + [(df'_k/dt) + 3(2\Delta + R_k)(df''_k/dt) - 2\bar{R}(df''_k/dt)] R_k \right\}, \end{aligned} \quad (4.6)$$

where the t -derivatives of $f_k(R)$ were given in Eq. (3.30). The first line in (4.6) will give the contributions to $\omega^n(u_*)$ while the second encodes the terms appearing in $\tilde{\omega}_m^n(u_*)$.

⁵A simple example illustrating this effect is the expansion $1/(1-10x) = \sum_n 10^n x^n$ where the expansion coefficients are determined by the pole at $x = 1/10$.

Moreover, Eq. (3.30) shows that (4.5) actually gives beta functions for the couplings u^n , $1 \leq n \leq N_{\text{prop}}$.

We can then evaluate the trace (4.5) using the zeroth order in the heat kernel and approximating the propagator by its expression at the fixed point u_* . The approximation in the heat-kernel expansion is again justified by the exponential growth of the series coefficients τ^n to which higher-order contributions of the heat-kernel are subleading. Solving for $\partial_t u^n$, this results in beta functions which are linear in the couplings u^n . The stability matrix is then obtained by taking the derivative with respect to these couplings. This results in the upper-triangular matrix. Thus the eigenvalues of B_*^{loc} are given by its diagonal entries. For example, $N_{\text{prop}} = 6$ leads to

$$B_*^{\text{loc}} = \begin{pmatrix} (-4.4 \times 10^{10} d_1 - 2.6 \times 10^{11}) & -3.68 \times 10^{16} & -243. & -1458. & -6561. & -2.53 \times 10^4 \\ 0 & -d_2 - 6 & 27 & 162 & 729 & \frac{19683}{7} \\ 0 & 0 & -d_3 - 6 & 12 & 54 & \frac{1458}{7} \\ 0 & 0 & 0 & -d_4 - 6 & 9 & \frac{243}{7} \\ 0 & 0 & 0 & 0 & -d_5 - 6 & \frac{54}{7} \\ 0 & 0 & 0 & 0 & 0 & -d_6 - 6 \end{pmatrix} \quad (4.7)$$

Notably, these contain the classical scaling dimension of the couplings. Thus one can indeed recover an almost classical scaling from (4.5). The specific structure of the regulator (3.22) is crucial for that, however.

This result also clarifies why the COE does not recover the almost-Gaussian scaling behavior. The localization mechanism owed to the pole in the propagator is still operational in this case. However, the regulator is no longer tied to the operators \mathcal{O}_n . In particular \mathcal{R}_k is independent of the anomalous scaling dimension. Thus, the mechanism leading to stability matrices of the form (4.7) fails in this case.

5 Discussion and Conclusions

Interacting renormalization group (RG) fixed points provide an attractive mechanism for providing a consistent and predictive high-energy completion of a theory beyond the realm of perturbation theory. The predictive power of such a fixed point is encoded in the spectrum of the stability matrix B_* , Eq. (1.2), controlling the linearized RG flow in its vicinity. The master equation derived in Eq. (2.21) encodes the general structure of this matrix separating the contributions originating from the classical scaling, quantum corrections, and regulator piece. This result is general in the sense that it holds for any fixed point irrespective of a given field content. Results obtained from the Wetterich equation and the composite operator equation can readily be cast into this parameterization. This highlights the structural differences occurring when evaluating the operator spectrum within these distinct computation schemes.

We then applied the general formalism to the Reuter fixed point projected on $f(R)$ -type interactions polynomial in the Ricci scalar R . The evaluation of the stability matrix

based on the Wetterich equation yields a spectrum of B_* which almost follows the canonical scaling for large powers of R . This is a key result supporting the predictive power of the Reuter fixed point. In the composite operator equation, this feature is absent though. Our general framework provides a comprehensive understanding of this mismatch in the following way: near the Reuter fixed point the regularized two-point function associated with the trace sector in the gravitational fluctuations exhibits a pole close to the expansion point of the functional renormalization group equations. This pole dominates the structure of the stability matrix for polynomials of sufficiently high order in R . The flow equations are well-approximated by the quantum contributions stemming from the trace-modes and the classical part of the stability matrix does not play any role. This mechanism is operative for both the Wetterich and the composite operator equation. The difference in the spectra of B_* can then be traced to the different regulator prescriptions. The regularization based on the Wetterich equation is constructed in such a way that also the dominant quantum contributions to the stability matrix exhibit classical scaling properties. For the composite operator equation this feature of the regulator and hence the almost-Gaussian scaling of the spectrum of B is absent. We stress that low-order expansions are unaffected by this mechanism though and shows qualitative agreement within the two complementary approaches.

Similar observations about the regulator dependence of the spectrum have recently been made in the context of functional $f(R)$ -truncations using non-adaptive regularization schemes [10, 50]. Studying the spectrum of admissible perturbations at a fixed functional $f_*(R)$ using Sturm-Liouville theory, it is found that the spectrum of B_* may either come with a finite or infinite number of relevant eigendirections, depending on the precise implementation of the regulator in the trace sector [50].

These findings raise the crucial question whether the almost-Gaussian scaling is indeed a genuine feature of the Reuter fixed point or a build-in feature of the key equation used to study it. One way to shed light on this question would be the study of $f(R)$ -type projections using an expansion based on an operator basis of the form $\{\mathcal{O}_n = \int d^d x \sqrt{g}(R-R_0)^n\}$, where the reference curvature R_0 is chosen in such a way that there are no propagator poles within the unit circle centered at the expansion point. Alternatively, a detailed understanding of the poles contained in $(\Gamma_k^{(2)} + \mathcal{R}_k)^{-1}$ on a generic, curved background spacetime may also give further information about the predictive power of the gravitational asymptotic safety program. This assessment also connects to the realm of functional $f(R)$ -truncations where the pole structure of $(\Gamma_k^{(2)} + \mathcal{R}_k)^{-1}$ also played a crucial role in obtaining isolated, global fixed functionals $f_k(R)$ by insisting that the solutions can pass through the poles of the flow equation located on the real axis [36, 81].

We note that the mechanism uncovered in this article may actually not be limited to the realm of quantum gravity. The interplay between poles of a two-point function and the spectrum of the stability matrix may be realized in other settings as well. Thus, the effect of quantum-induced almost-Gaussian scaling may occur much more frequently. Clearly, a general understanding of this situation would be highly desirable also beyond the realm of $f(R)$ -computations and we hope to come back to this in the future.

m	0	1	2	3	4	5	6
α_m^S	1	$\frac{1}{6}$	$\frac{29}{2160}$	$\frac{37}{54432}$	$\frac{149}{6531840}$	$\frac{179}{431101440}$	$-\frac{1387}{201755473920}$
α_m^{TT}	5	$-\frac{5}{6}$	$-\frac{1}{432}$	$\frac{311}{54432}$	$\frac{109}{1306368}$		

Table 2. Summary of the relevant deWitt coefficients for the Laplacian on a four-dimensional background sphere [82]. The coefficients not listed in the table do not enter into our computation.

Acknowledgements

We thank Martin Reuter, Carlo Pagani, Luca Buoninfante, and Rudrajit Banerjee for interesting discussions. MB gratefully acknowledges financial support by the Deutsche Forschungsgemeinschaft (DFG, German Research Foundation) – project number 493330310. The work of AK on the spectrum of the stability matrix is supported by the Russian Science Foundation grant No 23-12-00051, <https://rscf.ru/en/project/23-12-00051/>.

A Calculation of γ_n^m for the operator family $\{\int d^d x \sqrt{g} R^n\}$

This appendix collects the technical details entering into the evaluation of the operator traces in Eq. (3.32). The computation utilizes the heat-kernel technology reviewed in [34] and we outline the relevant steps in order to render the present work self-contained.

Inspecting the traces in Eq. (3.32), we see that their arguments are given by operator-valued functions $W_s(\Delta)$ where $\Delta := -\bar{g}^{\mu\nu} \bar{D}_\mu \bar{D}_\nu$ is the Laplacian constructed from the background metric and the trace is either over scalars ($s = S$) or transverse-traceless symmetric matrices ($s = \text{TT}$). Our computation tracks powers of the background scalar curvature \bar{R} only. Hence it suffices to work on a spherically symmetric background.

We then evaluate the traces using the early-time expansion of the heat kernel. Exploiting that we work on a background sphere, this expansion takes the form

$$\text{Tr}_s [W(\Delta)] = \frac{1}{(4\pi)^{d/2}} \sum_{m=0}^{\infty} \alpha_m^s Q_{\frac{d}{2}-m}[W] \int d^d x \sqrt{g} \bar{R}^m. \quad (\text{A.1})$$

Here α_m^s are the deWitt coefficients with $\bar{R} = 1$. For the background sphere these numbers can be found in [82] and we collect the relevant ones in Table 2. The Q -functionals are given in terms of the Mellin transform of the trace argument. For positive index $m > 0$,

$$Q_m[W] = \frac{1}{\Gamma(m)} \int_0^\infty dz z^{m-1} W(z). \quad (\text{A.2})$$

For $m \leq 0$ one can integrate by parts to obtain

$$Q_{-m}[W] = \frac{(-1)^k}{\Gamma(m+k)} \int_0^\infty dz z^{m+k-1} W^{(k)}(z), \quad m+k > 0. \quad (\text{A.3})$$

For $m + k$ being integer, this reduces to the relation $Q_{-m}[W] = (-1)^m W^{(m)}(0)$. Based on Eq. (A.2) one furthermore establishes the identity that

$$Q_m [z^p W] = \frac{\Gamma(m+p)}{\Gamma(m)} Q_{m+p}[W]. \quad (\text{A.4})$$

In order to transition to dimensionless quantities, we finally define

$$\begin{aligned} q_m^S &:= (k^2)^{-m-2} Q_m[W^S(\cdot; k^2 \rho)], \\ q_m^{\text{TT}} &:= (k^2)^{-m-1} Q_m[W^{\text{TT}}(\cdot; k^2 \rho)]. \end{aligned} \quad (\text{A.5})$$

Based on these prerequisites, we proceed by evaluating I_1 and I_2 . The composite operator Hessian $\mathcal{O}_n^{(2)}$ can be found in [62] and the propagator modalities are as in [34]. This results in the trace arguments

$$\begin{aligned} W^{\text{TT}}(\Delta; \bar{R}) &= \left[-\eta_{f'_k(\bar{R})} + \partial_t \right] R_k, \\ W^S(\Delta; \bar{R}) &= 4 \left(\partial_t R_k + \zeta_{f_k(\bar{R})} R_k \right) [(d-1)\Delta - \bar{R}] \\ &\quad + 2(d-1)R_k \left[2\partial_t R_k + \zeta_{f_k(\bar{R})} R_k \right] + (d-2) \frac{f'_k(\bar{R})}{f''_k(\bar{R})} \left[\partial_t R_k - \eta_{f_k(\bar{R})} R_k \right]. \end{aligned} \quad (\text{A.6})$$

Here we specialized to the Litim-type cutoff (3.2) and introduced the anomalous dimensions

$$\begin{aligned} \eta_{f_k(R)} &= -\frac{1}{f'_k(R)} \partial_t f'_k(R) = -(d-2) - \frac{(\partial_t \mathcal{F}'_k)(\rho)}{\mathcal{F}'_k(\rho)} + 2\rho \frac{\mathcal{F}''_k(\rho)}{\mathcal{F}'_k(\rho)}, \\ \zeta_{f_k(R)} &= \frac{1}{f''_k(R)} \partial_t f''_k(R) = (d-4) + \frac{(\partial_t \mathcal{F}''_k)(\rho)}{\mathcal{F}''_k(\rho)} - 2\rho \frac{\mathcal{F}'''_k(\rho)}{\mathcal{F}''_k(\rho)}. \end{aligned} \quad (\text{A.7})$$

Using the operator insertion $\mathcal{O}_n = \int d^d x \sqrt{g} R^n$, the two traces in Eq. (3.32) evaluate to

$$\begin{aligned} I_1 &= \frac{1}{(4\pi)^{d/2}} \mathcal{F}'_k(\rho) \rho^{n-1} \left(\mathcal{F}'_k(\rho) \left(1 - \frac{2(d-2)}{d(d-1)} \rho \right) + \mathcal{F}_k(\rho) \right)^{-2} \\ &\quad \times \left\{ \frac{d}{2} c_1^{\text{TT}} \alpha_0^{\text{TT}} q_{\frac{d}{2}+1}^{\text{TT}} + \sum_{m=0}^{\infty} \left(c_0^{\text{TT}} \rho \alpha_m^{\text{TT}} + c_1^{\text{TT}} (d/2 - m - 1) \alpha_{m+1}^{\text{TT}} \right) q_{\frac{d}{2}-m}^{\text{TT}} \right\} \end{aligned} \quad (\text{A.8})$$

and

$$\begin{aligned}
I_2 = & \frac{(1-d)}{(4\pi)^{d/2}} \mathcal{F}_k''(\rho) \rho^{n-2} \left\{ 2(d-1)^2 \mathcal{F}_k''(\rho) \left[1 - \frac{\rho}{d-1} \right]^2 \right. \\
& \left. + (d-1)(d-2) \mathcal{F}_k'(\rho) \left[1 - \frac{\rho}{d-1} \right] - (d-2)\rho \mathcal{F}_k'(\rho) + \frac{d(d-2)}{2} \mathcal{F}_k(\rho) \right\}^{-2} \\
& \times \left\{ \frac{d}{2} \left[c_1^S \alpha_0^S \rho + \left(\frac{d}{2} - 1 \right) c_2^S \alpha_1^S \right] q_{\frac{d}{2}+1}^S + \frac{d}{2} \left(\frac{d}{2} + 1 \right) c_2^S \alpha_0^S q_{\frac{d}{2}+2}^S \right. \\
& \left. + \sum_{m=0}^{\infty} \left[c_0^S \alpha_m^S \rho^2 + \left(\frac{d}{2} - m - 1 \right) c_1^S \alpha_{m+1}^S \rho \right. \right. \\
& \left. \left. + \left(\frac{d}{2} - m - 2 \right) \left(\frac{d}{2} - m - 1 \right) c_2^S \alpha_{m+2}^S \right] q_{\frac{d}{2}-m}^S \right\}.
\end{aligned} \tag{A.9}$$

The coefficients c^S depend on d and n and are given by

$$\begin{aligned}
c_0^{\text{TT}} &= \frac{n(d-2)}{d(d-1)} - \frac{1}{2}, & c_0^S &= \frac{d(d-2)}{4} - n(d-n-1), \\
c_1^{\text{TT}} &= -n/2, & c_1^S &= \frac{n(d^2 - (4n-1)(d-1) - 1)}{2}, \\
& & c_2^S &= n(n-1)(d-1)^2.
\end{aligned} \tag{A.10}$$

In principle, one can now expand Eqs. (A.8) and (A.9) in powers of ρ and subsequently read off $\gamma_n^m(u(k))$ according to Eq. (3.32). Owing to the k -derivatives acting on the couplings $u(k)$ in the second term of the anomalous dimensions (A.7) the resulting system is not self-contained though and requires an explicit expression for the beta functions $\partial_t u^n(k) = \beta^n(u)$. At a fixed point u^* the beta functions vanish by definition. This entails that

$$\mathcal{F}_k(\rho) \rightarrow \mathcal{F}_*(\rho) = \sum_{n=0}^{N_{\text{prop}}} u_*^n \rho^n, \quad (\partial_t \mathcal{F}_*)(\rho) = 0. \tag{A.11}$$

Substituting these conditions into the expressions for the anomalous dimensions gives

$$\begin{aligned}
\eta_{f_k(R)} &\rightarrow \eta_*(\rho) = -(d-2) + 2\rho \frac{\mathcal{F}_*''(\rho)}{\mathcal{F}_*'(\rho)}, \\
\zeta_{f_k(R)} &\rightarrow \zeta_*(\rho) = (d-4) - 2\rho \frac{\mathcal{F}_*'''(\rho)}{\mathcal{F}_*''(\rho)}.
\end{aligned} \tag{A.12}$$

By substituting the fixed point values u_* , given in Eq. (3.31), the results (A.8) and (A.9) allow to give the scaling dimension $\gamma_n^m(u_*)$ at the fixed point.

B The flow equation for functional $f(R)$ -truncations

For completeness, we reproduce the functional f(R)-equation obtained in [33].

$$\begin{aligned}
384\pi^2 (\partial_t \mathcal{F}_k + 4\mathcal{F}_k - 2\rho \mathcal{F}'_k) = & \\
& \left[5\rho^2 \theta \left(1 - \frac{\rho}{3}\right) - \left(12 + 4\rho - \frac{61}{90} \rho^2\right) \right] \left[1 - \frac{\rho}{3}\right]^{-1} + 10\rho^2 \theta \left(1 - \frac{\rho}{3}\right) \\
& + \left[10\rho^2 \theta \left(1 - \frac{\rho}{4}\right) - \rho^2 \theta \left(1 + \frac{\rho}{4}\right) - \left(36 + 6\rho - \frac{67}{60} \rho^2\right) \right] \left[1 - \frac{\rho}{4}\right]^{-1} \\
& + \left[\eta_f \left(10 - 5\rho - \frac{271}{36} \rho^2 + \frac{7249}{4536} \rho^3\right) + \left(60 - 20\rho - \frac{271}{18} \rho^2\right) \right] \left[1 + \frac{\mathcal{F}_k}{\mathcal{F}'_k} - \frac{\rho}{3}\right]^{-1} \\
& + \frac{5\rho^2}{2} \left[\eta_f \left(\left(1 + \frac{\rho}{3}\right)\theta\left(1 + \frac{\rho}{3}\right) + \left(2 + \frac{\rho}{3}\right)\theta\left(1 + \frac{\rho}{6}\right)\right) + 2\theta\left(1 + \frac{\rho}{3}\right) + 4\theta\left(1 + \frac{\rho}{6}\right) \right] \left[1 + \frac{\mathcal{F}_k}{\mathcal{F}'_k} - \frac{\rho}{3}\right]^{-1} \\
& + \left[\mathcal{F}'_k \eta_f \left(6 + 3\rho + \frac{29}{60} \rho^2 + \frac{37}{1512} \rho^3\right) + (\partial_t \mathcal{F}_k'' - 2\rho \mathcal{F}_k''') \left(27 - \frac{91}{20} \rho^2 - \frac{29}{30} \rho^3 - \frac{181}{3360} \rho^4\right) \right. \\
& \left. + \mathcal{F}_k'' \left(216 - \frac{91}{5} \rho^2 - \frac{29}{15} \rho^3\right) + \mathcal{F}'_k \left(36 + 12\rho + \frac{29}{30} \rho^2\right) \right] \left[2\mathcal{F}_k + 3\mathcal{F}'_k \left(1 - \frac{2}{3}\rho\right) + 9\mathcal{F}_k'' \left(1 - \frac{\rho}{3}\right)^2\right]^{-1}, \tag{B.1}
\end{aligned}$$

where we used the short-hand notation

$$\eta_f = \frac{1}{\mathcal{F}'_k} (\partial_t \mathcal{F}'_k + 2\mathcal{F}'_k - 2\rho \mathcal{F}_k''). \tag{B.2}$$

This equation forms the basis for evaluating B_*^{FRGE} in Sec. 3.2.

References

- [1] Gerard 't Hooft and M. J. G. Veltman. One loop divergencies in the theory of gravitation. *Annales Poincare Phys. Theor.*, A20:69–94, 1974.
- [2] Marc H. Goroff and Augusto Sagnotti. Quantum Gravity at Two Loops. *Phys. Lett.*, B160:81, 1985. doi:10.1016/0370-2693(85)91470-4.
- [3] Marc H. Goroff and Augusto Sagnotti. The Ultraviolet Behavior of Einstein Gravity. *Nucl. Phys.*, B266:709, 1986. doi:10.1016/0550-3213(86)90193-8.
- [4] A. E. M. van de Ven. Two loop quantum gravity. *Nucl. Phys.*, B378:309–366, 1992. doi:10.1016/0550-3213(92)90011-Y.
- [5] John F. Donoghue, Mikhail M. Ivanov, and Andrey Shkerin. EPFL Lectures on General Relativity as a Quantum Field Theory. 2017. arXiv:1702.00319.
- [6] Frank Saueressig. *The Functional Renormalization Group in Quantum Gravity*. 2023. arXiv:2302.14152, doi:10.1007/978-981-19-3079-9_16-1.
- [7] Jan M. Pawłowski and Manuel Reichert. Quantum Gravity from dynamical metric fluctuations. 9 2023. arXiv:2309.10785.
- [8] Astrid Eichhorn and Marc Schiffer. Asymptotic safety of gravity with matter. 12 2022. arXiv:2212.07456.
- [9] Benjamin Knorr, Chris Ripken, and Frank Saueressig. Form Factors in Asymptotically Safe Quantum Gravity. 10 2022. arXiv:2210.16072.

- [10] Tim R. Morris and Dalius Stulga. *The Functional $f(R)$ Approximation*. 2023. [arXiv:2210.11356](#), [doi:10.1007/978-981-19-3079-9_19-1](#).
- [11] Riccardo Martini, Gian Paolo Vacca, and Omar Zanusso. Perturbative approaches to non-perturbative quantum gravity. 10 2022. [arXiv:2210.13910](#), [doi:10.1007/978-981-19-3079-9_25-1](#).
- [12] C. Wetterich. Quantum gravity and scale symmetry in cosmology. 11 2022. [arXiv:2211.03596](#).
- [13] Alessia Platania. Black Holes in Asymptotically Safe Gravity. 2 2023. [arXiv:2302.04272](#).
- [14] Robert Percacci. *An Introduction to Covariant Quantum Gravity and Asymptotic Safety*, volume 3 of *100 Years of General Relativity*. World Scientific, 2017. [doi:10.1142/10369](#).
- [15] Martin Reuter and Frank Saueressig. *Quantum Gravity and the Functional Renormalization Group*. Cambridge University Press, 2019.
- [16] Martin Reuter. Nonperturbative evolution equation for quantum gravity. *Phys. Rev. D*, 57:971–985, 1998. [arXiv:hep-th/9605030](#), [doi:10.1103/PhysRevD.57.971](#).
- [17] O. Lauscher and M. Reuter. Flow equation of quantum Einstein gravity in a higher derivative truncation. *Phys. Rev. D*, 66:025026, 2002. [arXiv:hep-th/0205062](#), [doi:10.1103/PhysRevD.66.025026](#).
- [18] Dario Benedetti, Pedro F. Machado, and Frank Saueressig. Asymptotic safety in higher-derivative gravity. *Mod. Phys. Lett. A*, 24:2233–2241, 2009. [arXiv:0901.2984](#), [doi:10.1142/S0217732309031521](#).
- [19] Dario Benedetti, Kai Groh, Pedro F. Machado, and Frank Saueressig. The Universal RG Machine. *JHEP*, 06:079, 2011. [arXiv:1012.3081](#), [doi:10.1007/JHEP06\(2011\)079](#).
- [20] Dario Benedetti. On the number of relevant operators in asymptotically safe gravity. *EPL*, 102(2):20007, 2013. [arXiv:1301.4422](#), [doi:10.1209/0295-5075/102/20007](#).
- [21] Juergen A. Dietz, Tim R. Morris, and Zoe H. Slade. Fixed point structure of the conformal factor field in quantum gravity. *Phys. Rev. D*, 94(12):124014, 2016. [arXiv:1605.07636](#), [doi:10.1103/PhysRevD.94.124014](#).
- [22] Holger Gies, Benjamin Knorr, Stefan Lippoldt, and Frank Saueressig. Gravitational Two-Loop Counterterm Is Asymptotically Safe. *Phys. Rev. Lett.*, 116(21):211302, 2016. [arXiv:1601.01800](#), [doi:10.1103/PhysRevLett.116.211302](#).
- [23] Tobias Denz, Jan M. Pawłowski, and Manuel Reichert. Towards apparent convergence in asymptotically safe quantum gravity. *Eur. Phys. J. C*, 78(4):336, 2018. [arXiv:1612.07315](#), [doi:10.1140/epjc/s10052-018-5806-0](#).
- [24] Kevin Falls, Callum R. King, Daniel F. Litim, Kostas Nikolakopoulos, and Christoph Rahmede. Asymptotic safety of quantum gravity beyond Ricci scalars. *Phys. Rev. D*, 97(8):086006, 2018. [arXiv:1801.00162](#), [doi:10.1103/PhysRevD.97.086006](#).
- [25] N. Ohta, R. Percacci, and A. D. Pereira. $f(R, R_{\mu\nu}^2)$ at one loop. *Phys. Rev. D*, 97(10):104039, 2018. [arXiv:1804.01608](#), [doi:10.1103/PhysRevD.97.104039](#).
- [26] Saswato Sen, Christof Wetterich, and Masatoshi Yamada. Asymptotic freedom and safety in quantum gravity. *JHEP*, 03:130, 2022. [arXiv:2111.04696](#), [doi:10.1007/JHEP03\(2022\)130](#).
- [27] Benjamin Knorr. The derivative expansion in asymptotically safe quantum gravity: general

- setup and quartic order. *SciPost Phys. Core*, 4:020, 2021. [arXiv:2104.11336](#), [doi:10.21468/SciPostPhysCore.4.3.020](#).
- [28] Alessio Baldazzi, Kevin Falls, Yannick Kluth, and Benjamin Knorr. Robustness of the derivative expansion in Asymptotic Safety. 12 2023. [arXiv:2312.03831](#).
- [29] Christof Wetterich. Exact evolution equation for the effective potential. *Phys. Lett. B*, 301:90–94, 1993. [arXiv:1710.05815](#), [doi:10.1016/0370-2693\(93\)90726-X](#).
- [30] Tim R. Morris. The Exact renormalization group and approximate solutions. *Int. J. Mod. Phys. A*, 9:2411–2450, 1994. [arXiv:hep-ph/9308265](#), [doi:10.1142/S0217751X94000972](#).
- [31] M. Reuter and C. Wetterich. Effective average action for gauge theories and exact evolution equations. *Nucl. Phys. B*, 417:181–214, 1994. [doi:10.1016/0550-3213\(94\)90543-6](#).
- [32] Alessandro Codello, Roberto Percacci, and Christoph Rahmede. Ultraviolet properties of f(R)-gravity. *Int. J. Mod. Phys. A*, 23:143–150, 2008. [arXiv:0705.1769](#), [doi:10.1142/S0217751X08038135](#).
- [33] Pedro F. Machado and Frank Saueressig. On the renormalization group flow of f(R)-gravity. *Phys. Rev. D*, 77:124045, 2008. [arXiv:0712.0445](#), [doi:10.1103/PhysRevD.77.124045](#).
- [34] Alessandro Codello, Roberto Percacci, and Christoph Rahmede. Investigating the Ultraviolet Properties of Gravity with a Wilsonian Renormalization Group Equation. *Annals Phys.*, 324:414–469, 2009. [arXiv:0805.2909](#), [doi:10.1016/j.aop.2008.08.008](#).
- [35] Dario Benedetti and Francesco Caravelli. The Local potential approximation in quantum gravity. *JHEP*, 06:017, 2012. [Erratum: *JHEP* 10, 157 (2012)]. [arXiv:1204.3541](#), [doi:10.1007/JHEP06\(2012\)017](#).
- [36] Juergen A. Dietz and Tim R. Morris. Asymptotic safety in the f(R) approximation. *JHEP*, 01:108, 2013. [arXiv:1211.0955](#), [doi:10.1007/JHEP01\(2013\)108](#).
- [37] Juergen A. Dietz and Tim R. Morris. Redundant operators in the exact renormalisation group and in the f(R) approximation to asymptotic safety. *JHEP*, 07:064, 2013. [arXiv:1306.1223](#), [doi:10.1007/JHEP07\(2013\)064](#).
- [38] I. Hamzaan Bridle, Juergen A. Dietz, and Tim R. Morris. The local potential approximation in the background field formalism. *JHEP*, 03:093, 2014. [arXiv:1312.2846](#), [doi:10.1007/JHEP03\(2014\)093](#).
- [39] Maximilian Demmel, Frank Saueressig, and Omar Zanusso. RG flows of Quantum Einstein Gravity on maximally symmetric spaces. *JHEP*, 06:026, 2014. [arXiv:1401.5495](#), [doi:10.1007/JHEP06\(2014\)026](#).
- [40] Maximilian Demmel, Frank Saueressig, and Omar Zanusso. RG flows of Quantum Einstein Gravity in the linear-geometric approximation. *Annals Phys.*, 359:141–165, 2015. [arXiv:1412.7207](#), [doi:10.1016/j.aop.2015.04.018](#).
- [41] Maximilian Demmel, Frank Saueressig, and Omar Zanusso. A proper fixed functional for four-dimensional Quantum Einstein Gravity. *JHEP*, 08:113, 2015. [arXiv:1504.07656](#), [doi:10.1007/JHEP08\(2015\)113](#).
- [42] K. Falls, D. F. Litim, K. Nikolakopoulos, and C. Rahmede. A bootstrap towards asymptotic safety. 1 2013. [arXiv:1301.4191](#).
- [43] Kevin Falls, Daniel F. Litim, Konstantinos Nikolakopoulos, and Christoph Rahmede. Further

- evidence for asymptotic safety of quantum gravity. *Phys. Rev. D*, 93(10):104022, 2016. [arXiv:1410.4815](#), [doi:10.1103/PhysRevD.93.104022](#).
- [44] Kevin Falls, Daniel F. Litim, Kostas Nikolakopoulos, and Christoph Rahmede. On de Sitter solutions in asymptotically safe $f(R)$ theories. *Class. Quant. Grav.*, 35(13):135006, 2018. [arXiv:1607.04962](#), [doi:10.1088/1361-6382/aac440](#).
- [45] Natália Alkofer and Frank Saueressig. Asymptotically safe $f(R)$ -gravity coupled to matter I: the polynomial case. *Annals Phys.*, 396:173–201, 2018. [arXiv:1802.00498](#), [doi:10.1016/j.aop.2018.07.017](#).
- [46] Natália Alkofer. Asymptotically safe $f(R)$ -gravity coupled to matter II: Global solutions. *Phys. Lett. B*, 789:480–487, 2019. [arXiv:1809.06162](#), [doi:10.1016/j.physletb.2018.12.061](#).
- [47] Nobuyoshi Ohta, Roberto Percacci, and Gian Paolo Vacca. Flow equation for $f(R)$ gravity and some of its exact solutions. *Phys. Rev. D*, 92(6):061501, 2015. [arXiv:1507.00968](#), [doi:10.1103/PhysRevD.92.061501](#).
- [48] Nobuyoshi Ohta, Roberto Percacci, and Gian Paolo Vacca. Renormalization Group Equation and scaling solutions for $f(R)$ gravity in exponential parametrization. *Eur. Phys. J. C*, 76(2):46, 2016. [arXiv:1511.09393](#), [doi:10.1140/epjc/s10052-016-3895-1](#).
- [49] Kevin Falls and Nobuyoshi Ohta. Renormalization Group Equation for $f(R)$ gravity on hyperbolic spaces. *Phys. Rev. D*, 94(8):084005, 2016. [arXiv:1607.08460](#), [doi:10.1103/PhysRevD.94.084005](#).
- [50] Alex Mitchell, Tim R. Morris, and Dalius Stulga. Provable properties of asymptotic safety in $f(R)$ approximation. *JHEP*, 01:041, 2022. [arXiv:2111.05067](#), [doi:10.1007/JHEP01\(2022\)041](#).
- [51] Astrid Eichhorn. The Renormalization Group flow of unimodular $f(R)$ gravity. *JHEP*, 04:096, 2015. [arXiv:1501.05848](#), [doi:10.1007/JHEP04\(2015\)096](#).
- [52] Sergio Gonzalez-Martin, Tim R. Morris, and Zoë H. Slade. Asymptotic solutions in asymptotic safety. *Phys. Rev. D*, 95(10):106010, 2017. [arXiv:1704.08873](#), [doi:10.1103/PhysRevD.95.106010](#).
- [53] Gustavo P. De Brito, Nobuyoshi Ohta, Antonio D. Pereira, Anderson A. Tomaz, and Masatoshi Yamada. Asymptotic safety and field parametrization dependence in the $f(R)$ truncation. *Phys. Rev. D*, 98(2):026027, 2018. [arXiv:1805.09656](#), [doi:10.1103/PhysRevD.98.026027](#).
- [54] Yannick Kluth and Daniel F. Litim. Fixed Points of Quantum Gravity and the Dimensionality of the UV Critical Surface. 8 2020. [arXiv:2008.09181](#).
- [55] Nicolai Christiansen, Kevin Falls, Jan M. Pawłowski, and Manuel Reichert. Curvature dependence of quantum gravity. *Phys. Rev. D*, 97(4):046007, 2018. [arXiv:1711.09259](#), [doi:10.1103/PhysRevD.97.046007](#).
- [56] Kevin G. Falls, Daniel F. Litim, and Jan Schröder. Aspects of asymptotic safety for quantum gravity. *Phys. Rev. D*, 99(12):126015, 2019. [arXiv:1810.08550](#), [doi:10.1103/PhysRevD.99.126015](#).
- [57] Yannick Kluth and Daniel F. Litim. Functional renormalization for $f(R_{\mu\nu\rho\sigma})$ quantum gravity. *Phys. Rev. D*, 106(10):106022, 2022. [arXiv:2202.10436](#), [doi:10.1103/PhysRevD.106.106022](#).

- [58] Jan M. Pawłowski. Aspects of the functional renormalisation group. *Annals Phys.*, 322:2831–2915, 2007. [arXiv:hep-th/0512261](#), [doi:10.1016/j.aop.2007.01.007](#).
- [59] Carlo Pagani and Martin Reuter. Composite Operators in Asymptotic Safety. *Phys. Rev. D*, 95(6):066002, 2017. [arXiv:1611.06522](#), [doi:10.1103/PhysRevD.95.066002](#).
- [60] Carlo Pagani. Note on scaling arguments in the effective average action formalism. *Phys. Rev. D*, 94(4):045001, 2016. [arXiv:1603.07250](#), [doi:10.1103/PhysRevD.94.045001](#).
- [61] W. Houthoff, A. Kurov, and F. Saueressig. On the scaling of composite operators in asymptotic safety. *JHEP*, 04:099, 2020. [arXiv:2002.00256](#), [doi:10.1007/JHEP04\(2020\)099](#).
- [62] Aleksandr Kurov and Frank Saueressig. On characterizing the Quantum Geometry underlying Asymptotic Safety. 3 2020. [arXiv:2003.07454](#).
- [63] Riccardo Martini, Dario Sauro, and Omar Zanusso. Composite higher derivative operators in $d = 2 + \epsilon$ dimensions and the spectrum of asymptotically safe gravity. 2 2023. [arXiv:2302.14804](#).
- [64] Maximilian Becker and Carlo Pagani. Geometric operators in the asymptotic safety scenario for quantum gravity. *Phys. Rev. D*, 99(6):066002, 2019. [arXiv:1810.11816](#), [doi:10.1103/PhysRevD.99.066002](#).
- [65] Maximilian Becker and Carlo Pagani. Geometric Operators in the Einstein–Hilbert Truncation. *Universe*, 5(3):75, 2019. [doi:10.3390/universe5030075](#).
- [66] Maximilian Becker, Carlo Pagani, and Omar Zanusso. Fractal Geometry of Higher Derivative Gravity. *Phys. Rev. Lett.*, 124(15):151302, 2020. [arXiv:1911.02415](#), [doi:10.1103/PhysRevLett.124.151302](#).
- [67] J. Laiho, S. Bassler, D. Du, J. T. Neelakanta, and D. Coumbe. Recent results in Euclidean dynamical triangulations. *Acta Phys. Polon. Supp.*, 10:317–320, 2017. [arXiv:1701.06829](#), [doi:10.5506/APhysPolBSupp.10.317](#).
- [68] J. Ambjorn, J. Jurkiewicz, and R. Loll. Emergence of a 4-D world from causal quantum gravity. *Phys. Rev. Lett.*, 93:131301, 2004. [arXiv:hep-th/0404156](#), [doi:10.1103/PhysRevLett.93.131301](#).
- [69] R. Loll. Quantum Gravity from Causal Dynamical Triangulations: A Review. *Class. Quant. Grav.*, 37(1):013002, 2020. [arXiv:1905.08669](#), [doi:10.1088/1361-6382/ab57c7](#).
- [70] Joren Brunekreef, Andrzej Görlich, and Renate Loll. Simulating CDT quantum gravity. 10 2023. [arXiv:2310.16744](#).
- [71] Tobias Hellwig, Andreas Wipf, and Omar Zanusso. Scaling and superscaling solutions from the functional renormalization group. *Phys. Rev. D*, 92(8):085027, 2015. [arXiv:1508.02547](#), [doi:10.1103/PhysRevD.92.085027](#).
- [72] Daniel F. Litim. Optimized renormalization group flows. *Phys. Rev. D*, 64:105007, 2001. [arXiv:hep-th/0103195](#), [doi:10.1103/PhysRevD.64.105007](#).
- [73] M. Reuter and Frank Saueressig. Renormalization group flow of quantum gravity in the Einstein–Hilbert truncation. *Phys. Rev. D*, 65:065016, 2002. [arXiv:hep-th/0110054](#), [doi:10.1103/PhysRevD.65.065016](#).
- [74] O. Lauscher and M. Reuter. Ultraviolet fixed point and generalized flow equation of

- quantum gravity. *Phys. Rev. D*, 65:025013, 2002. [arXiv:hep-th/0108040](#), [doi:10.1103/PhysRevD.65.025013](#).
- [75] Daniel F. Litim. Fixed points of quantum gravity. *Phys. Rev. Lett.*, 92:201301, 2004. [arXiv:hep-th/0312114](#), [doi:10.1103/PhysRevLett.92.201301](#).
- [76] Holger Gies, Benjamin Knorr, and Stefan Lippoldt. Generalized Parametrization Dependence in Quantum Gravity. *Phys. Rev. D*, 92(8):084020, 2015. [arXiv:1507.08859](#), [doi:10.1103/PhysRevD.92.084020](#).
- [77] James W. York, Jr. Covariant decompositions of symmetric tensors in the theory of gravitation. *Ann. Inst. H. Poincaré Phys. Theor.*, 21:319–332, 1974.
- [78] Jr. York, James W. Conformally invariant orthogonal decomposition of symmetric tensors on Riemannian manifolds and the initial-value problem of general relativity. *Journal of Mathematical Physics*, 14(4):456–464, April 1973. [doi:10.1063/1.1666338](#).
- [79] S. Carlip. Dimension and Dimensional Reduction in Quantum Gravity. *Universe*, 5:83, 2019. [arXiv:1904.04379](#), [doi:10.3390/universe5030083](#).
- [80] Martin Reuter and Frank Saueressig. Asymptotic Safety, Fractals, and Cosmology. *Lect. Notes Phys.*, 863:185–223, 2013. [arXiv:1205.5431](#), [doi:10.1007/978-3-642-33036-0_8](#).
- [81] Maximilian Demmel, Frank Saueressig, and Omar Zanusso. Fixed-Functionals of three-dimensional Quantum Einstein Gravity. *JHEP*, 11:131, 2012. [arXiv:1208.2038](#), [doi:10.1007/JHEP11\(2012\)131](#).
- [82] Yannick Kluth and Daniel F. Litim. Heat kernel coefficients on the sphere in any dimension. *Eur. Phys. J. C*, 80(3):269, 2020. [arXiv:1910.00543](#), [doi:10.1140/epjc/s10052-020-7784-2](#).